論文 / 著書情報
Article / Book Information

題目(和文)	
Title(English)	Conversion of red mud (bauxite residue) into heterogeneous base catalyst for biodiesel production
著者(和文)	AgusWahyudi
Author(English)	Agus Wahyudi
出典(和文)	学位:博士(工学), 学位授与機関:東京工業大学, 報告番号:甲第10696号, 授与年月日:2017年12月31日, 学位の種別:課程博士, 審査員:日野出 洋文,江頭 竜一,MARIQUIT EDEN GAN,吉川 邦夫,高橋 史武
Citation(English)	Degree:Doctor (Engineering), Conferring organization: Tokyo Institute of Technology, Report number:甲第10696号, Conferred date:2017/12/31, Degree Type:Course doctor, Examiner:,,,,
学位種別(和文)	博士論文
Type(English)	Doctoral Thesis

Conversion of red mud (bauxite residue) into heterogeneous base catalyst for biodiesel production

A dissertation submitted to
TOKYO INSTITUTE OF TECHNOLOGY
for the degree of

DOCTOR OF ENGINEERING

by
AGUS WAHYUDI

Department of International Development Engineering
Graduate School of Science and Engineering

August 2017

Table of Contents

List of Figures

List of Tables

Chapter 1

Introduction

This chapter provides a background of problem in the waste of alumina industry, namely red mud, and the potential utilization of this waste as a catalyst for biodiesel production. Literature review, potential improvements of red mud, and the objectives of this study are presented in this chapter.

1.1 Red mud

Red mud is a reddish brown coloured solid waste generated during the processing of bauxite, the most common ore of aluminium [1,2]. In 1888, Karl Josef Bayer developed and patented the Bayer process for the production of alumina from bauxite [3]. The ore is washed, ground and dissolved in sodium hydroxide solution under heat and pressure. The resulting products are sodium aluminate liquor, that goes for further processing to produce alumina and a large quantity of undissolved solid waste called red mud or bauxite residue [4]. **Fig. 1.1** shows material balance of alumina production through the Bayer process [5]. For every ton alumina produced, the process generates one to two tonnes of red mud as by-product [6].

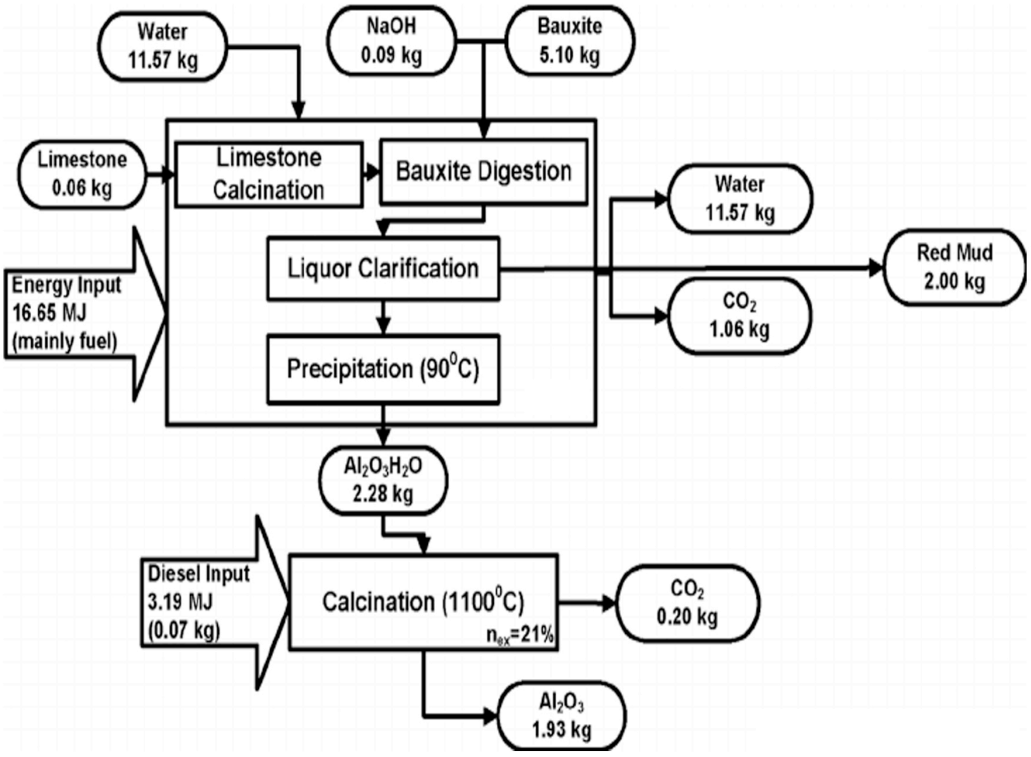

Fig. 1.1. Material balance of Bayer process in alumina industry [5]

Globally, the total amount of red mud produced every year is between 60 and 120 million tonnes [7]. According to the European List of Waste, red mud is not categorized as hazardous waste [8]. However, it is not guaranteed in the future effect, its effect to the environment especially in large quantities. The alkaline nature and the oxides/minerals content in red mud can cause environmental problems and leading to the contamination of ground water under severe conditions [9].

The disposal of red mud remains a major problem. Generally it is disposed in tailing pond or dumped in the sea. Australia, China, India, and Germany were reported to dispose this waste in the tailing pond, as shown in **Fig. 1.2**. The slurry has a composition of 45% liquid and 55% solids [10]. While in Japan, the majority of red mud is dumped into the ocean after neutralization. Aluminum manufacturing companies in Japan have already developed pretreatment techniques for bauxite

before the Bayer process to reduce the amount of red mud discharged [11]. Globally, the total amount of red mud produced every year is between 60 and 120 million tonnes [7].

Fig. 1.2. Red mud disposal [12]

The spill of red mud reservoir at the Ajka alumina plant in Hungary in 2010 is warning us to pay attention in the management of wastes and in the handling of complex environmental problems [7]. From this accident, about one million cubic meters of sludge spread out around 40 km^2. At least nine people died, 150 are injured, and it forced about 500 residents to evacuate [13]. **Fig. 1.3** shows the situation surround Ajka alumina reservoir during the accident.

Fig. 1.3. Photos of alumina plant accident in Hungary [13]

1.1.1 Characteristics

Red mud is highly alkaline with the pH ranging from 10 to 12. Due to its highly caustic nature, it is considered hazardous to the environment, therefore necessitating particular treatments [14,15]. Red mud has a fine particle size distribution with 90% by volume below the size of 75 mm [16]. **Fig. 1.4** shows a picture of red mud after water evaporation.

Fig. 1.4. Red mud after water evaporation [17]

Red mud consists of a mixture of minerals originally present in the parent mineral, such as hematite (Fe_2O_3), goethite (FeOOH), iron hydroxide ($Fe(OH)_3$), magnetite (Fe_3O_4), rutile (TiO_2), anatase (TiO_2), bayerite ($Al(OH)_3$), halloysite ($Al_2Si_2O_5(OH)_4$), boehmite (AlO(OH)), diaspore (AlO(OH)), gibbsite ($Al(OH)_3$), quartz (SiO_2), and calcite ($CaCO_3$) [4,9]. The chemical analysis reveals that red mud contains main constituents include Fe_2O_3, Al_2O_3, SiO_2, Na_2O, CaO, MgO, TiO_2 and a number of minor constituents such as K, Cr, V, Ni, Cu, Mn, Zn, and rare earth elements [1,14,18]. Generally ferric oxide (Fe_2O_3) is the major constituent of red mud and gives it its characteristic reddish brown colour [4]. **Table 1.1** presents typical chemical composition of red mud.

Table 1.1. Typical chemical composition of red mud [17]

Chemical composition	Wt%
Fe_2O_3	30-60
Al_2O_3	10-20
SiO_2	3-50
Na_2O	2-10
CaO	2-8
TiO_2	trace-25

1.1.2 Potential applications

According to the physical and chemical properties, red mud will be a valuable secondary resources when it is managed properly [19]. By utilizing this low-cost waste materials, not only the process could be made economical, but also an environmentally friendly process could be promoted. **Table 1.2** presents the potential utilizations of red mud.

Table 1.2. Potential applications of red mud

Aspect	Application	Reference
Building and structural materials	Bricks	[20,21]
	Cement	[22,23]
	Ceramic materials	[24–26]
Water treatment	Phenol removal	[27]
	Heavy metal removal	[28–30]
	Nitrate removal	[31]
	Phosphate removal	[32]
	Dye colour removal	[33]
Metal recovery	Fe, Al, Na	[34–38]
	Sc, Y, La, Ti, V	[39–41]
Catalyst	Hydrogenation and liquefaction	[42–44]
	Hydrodechlorination reaction	[45,46]
	Exhaust gas clean-up	[47]
Others	Pigments and paints	[48–50]
	Soil and mine site remediation	[51,52]

1.2 Biodiesel

Biodiesel is a promising renewable energy. It has many advantages for alternative fuel due to its characteristics, such as biodegradability, renewability and lower emissions [53–55]. Biodiesel is a mixture of alkyl esters and it can be used in existing diesel engines, without any modification [56,57]. So far, this alternative fuel has been successfully produced by transesterification of vegetable oils, such as corn, cottonseed, canola, palm, soybean, and sunflower, using basic catalysts [58,59].

1.2.1 Transesterification reaction

The common way to produce biodiesel is by transesterification of triglycerides of plant oil using alcohol, in presence of basic catalyst [60]. The alcohol used for

transesterification is usually methanol. The general scheme of the trasesterification reaction is presented in **Fig. 1.5**, where R is a mixture of various fatty acid chains.

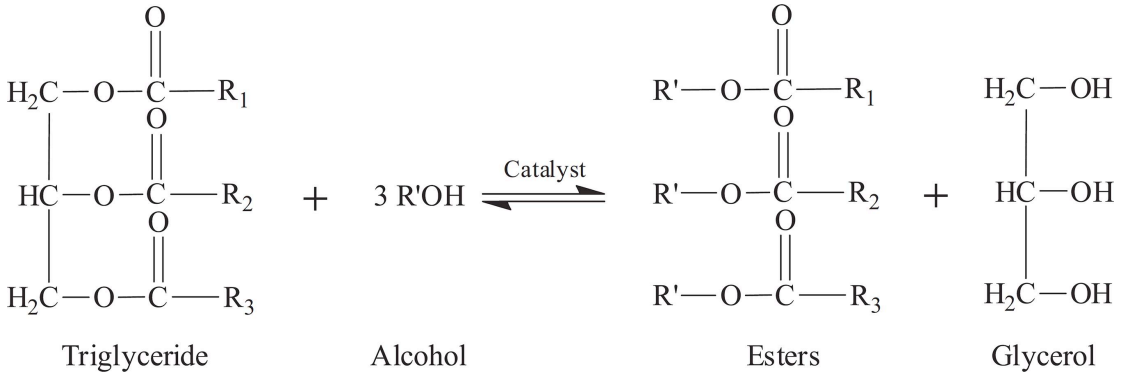

Fig. 1.5. Scheme of transesterification of triglyceride [61]

The stoichiometry of the reaction is 3:1 molar ratio of alcohol to oil, to produce 3 mol of alkyl esters and 1 mol glycerol. However, in practice it is usually used from 6:1 to 1000:1 to to shift the equilibrium of the reaction to produce more alkyl esters [62,63]. Complete conversion of the triglyceride involves three reactions with monoglyceride and diglyceride intermediates which are reversible reactions as shown in **Fig. 1.6** [58].

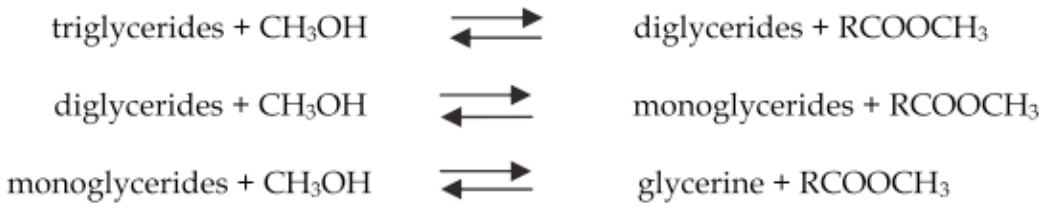

Fig. 1.6. Scheme of complete conversion of triglyceride in transesterification reaction [58]

The transesterification reaction produces two liquid phases: alkyl esters and glycerol. Using funnel separator, glycerol is collected at the bottom after some time of

settling. Phase separation can be observed within short time and can be completed within 2 to 20 h, when the reaction is carried out at laboratory scale [64].

1.2.2 Biodiesel catalyst

One of the important factors to produce biodiesel is the role of catalyst. Base catalysts play an important role to deprotonate methanol into methoxide ion ($^{-}OCH_3$), a nucleophilic species. This species can easily attacks trygliceride molecules to produce methyl esters (biodiesel) [65,66]. **Fig. 1.7** shows the reaction mechanism between alkoxide ion and triglyceride to produce alkyl ester [67]

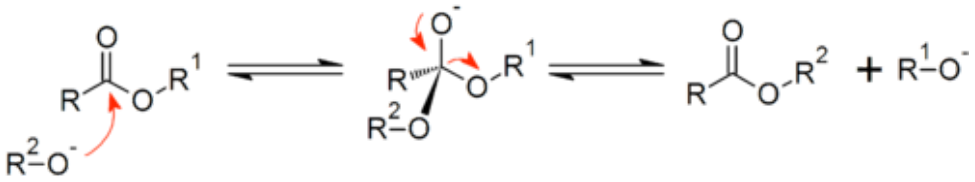

Fig. 1.7. Mechanism of reaction between alkoxide ion and triglyceride to produce alkyl ester [67]

The transesterification reaction can be carried out either by presence of homogeneous or heterogeneous catalysts (**Table 1.3**). The homogeneous catalysts, such as sodium and potassium hydroxide, carbonates, sodium and potassium alkoxides, have been commercially used for biodiesel production with very high efficiency [68,69]. However, these catalysts have some limitations, such as difficulties in separation from the mixtures, resulting in large amount of wastewater for neutralization and low reusability [70].

To overcome these problems, heterogeneous or solid catalysts were introduced. These types of catalysts have some advantages, such as high separability from mixture, reusability, and being environmentally benign due to fewer disposal problems [58,71–73]. Besides, heterogeneous catalysts exhibit a less corrosive

character and can be used in a fixed-bed reactor, leading to safer, cheaper and more environment-friendly operation [74].

Table 1.3. Performance of homogeneous and heterogeneous catalyst for biodiesel production [73]

Catalyst	Advantages	Disadvantages
Homogeneous (Liquid catalyst)	High reaction efficiency	• Difficulties in separation from the mixtures • Low reusability
Heterogeneous (Solid catalyst)	• Easy to separate from the mixtures • Reusable	The reaction efficiency is not so high

The most commonly studied heterogeneous basic catalysts are alkaline earth metal carbonates ($CaCO_3$), alkaline earth metal oxides (CaO, MgO, SrO, BaO) and other oxides as ZnO [60,62,63,68,74]. Among the above-mentioned oxide, the CaO is the most extensively studied in the transesterification reaction. The catalytic activity of CaO has been compared with other calcium compounds (calcium hydroxide and calcium alkoxides) at the same reaction conditions. The reactivity order is $Ca(OH)_2$<CaO<$Ca(CH_3O)$. This is corresponding with Lewis theory: the methoxides of alkaline-earth metals are more basic than their oxides and these are more basic than their hydroxides [75,76]. Besides that, alkaline metals in silicate and aluminate form ($NaAlO_2$ and $Na_2Si_2O_5$) were also introduced as solid catalyst for biodiesel production. Sodium aluminate and sodium silicate have proven to show activity as solid catalyst for the transesterification reaction. Those materials had high basicity and high efficiency for biodiesel production [77,78].

Furthermore, research on the development of solid catalysts have attracted attention to being explored, especially from the view point of the application of waste

materials. The solid catalysts synthesized from waste materials, such as waste aluminium foil [79], mud clam shell [80], sugarcane press mud [81], and coconut husk ash [82] have been developed to promote biodiesel production. By using those low-cost waste materials, not only the process could be made economical, but also an environmentally friendly process also could be promoted.

1.2.3 Deactivation of solid catalyst

Heterogeneous catalysts have attracted an attention to be used in industries due to some advantages compare to homogeneous catalysts [72]. Since it exists in different phase from the mixtures, heterogeneous or solid catalyst can easily be separated and reused [73]. However, the activity of the used catalyst is generally lower than the fresh one [83].

In biodiesel production, the deactivation of solid catalyst often occurs and it is caused by some factors, such as leaching of active sites, strutural collapse, and surface poisoning by contaminants [84]. Kouzo et al. reported that some soluble substances were leached out from the CaO solid base catalyst during the transesterification reaction [85]. The alkali metals from the catalyst easily react with esters and trglycerides to form soaps, which signicantly leads to the deactivation of the catalyst [72,86].

Another factor of catalyst deactivaton is structural collapse. Porous catalysts have attracted an attention for biodiesel production due to these materials offer a large accessibility of catalyst surface area for reaction. However, the porous structure of the catalyst can be collapsed by high temperature or mechanical mixing during reaction [87,88].

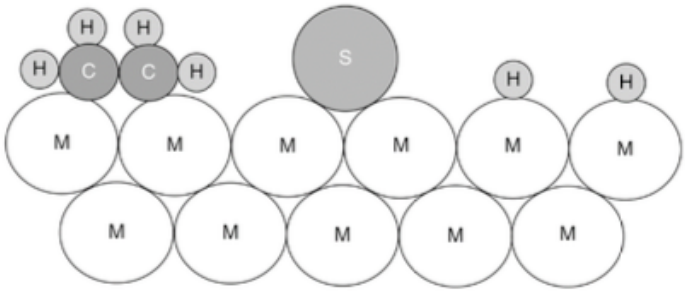

Fig. 1.8. Conceptual model of poisoning a metal surface catalyst by contaminants [83]

The next reason behind the catalyst deactivation is surface poisoning by contaminants. The contaminants are organic compounds from the products or by-products of the transesterification reaction, such as methyl esters, glycerol or diglyceride [63]. The contaminants attach on the catalyst surface, fill the pore, and cover the active sites of the catalyst, as shown in **Fig. 1.8.** Such conditions led to the low accessibility of the active sites of metal oxides to the reactants, which significantly inibit the activity of the catalyst [84].

1.2.4 Instrumentation for catalyst analysis

A comprehensive study of catalyst deactivation mechanism will help to plan its regeneration process in biodiesel production. Therefore, a wide range of analytical techniques for catalyst characterization were used, such as X-ray diffraction (XRD), Fourier transform infrared (FTIR) spectroscopy, scanning electron microscope (SEM), Brunauer-Emmett-Teller (BET) calculation, thermogravimetry and differential thermal analysis (TG-DTA), Hammett indicator, and inductively coupled plasma-atomic emission spectrometric (ICP-AES) [84].

XRD is the most common technique to analyze crystalline material because it allows the identification of crystalline phases in bulk materials from diffraction peak characteristics [89,90]. According to the XRD profiles, some information can be

obtained such as crystalline phases variation, evolution of active phase concentration, and surface poisoning due to contaminants during reaction.

FTIR spectroscopy is used to disclose the structure change of the used catalyst during reaction [91,92]. The FTIR results show that the fresh catalyst is different from those collected after reaction. The used catalyst presents new bands, which could be assigned to the product of the reaction, such as methyl esters and glycerol [93].

SEM is used to provide high-resolution image of the surface of a catalyst, which give morphology information of the fresh and used catalyst surface. Ho et al. reported that the fresh catalyst had shown uniform distribution of agglomerates, while after reaction, the catalyst appeared to be more condensed mass [94].

BET theory is used to explain the physical adsoption-desorption of nitrogen on a solid surface and provide analysis to measure specific surface area and pore size distribution of the material [95]. Researchers have investigated the reason behind the loss in catalytic activity from the fresh to deactivated catalyst using BET. The BET showed that the loss in catalytic activity could be related to the decrease of the BET surface area, a decrease of pore volume, and an increase of pore diameter of the used catalyst [96].

TG-DTA provides information of thermal behavior of the materials. Wen et al. used TG-DTA to investigate the degradation of catalytic activity of the catalyst after the first use. The results showed that a weight loss occurred at 423−773 K with an exothermic peak at 603 K. This peak corresponds to the decomposition of organic compounds, indicating that the surfaces and pores of the catalyst are filled by organic species, such as methyl esters and glycerol [95].

Hammett indicators is usually used to measure the basic strength of the catalyst [97]. This method is based on the change in color of acid-base indicators.

Basicity or total basic site density over solid catalyst is the number of exposed basic sites per unit mass. Usually, the basicity is shown to be closely related to the catalytic activity. Silva et al. compared the basicity of the fresh and reused Hydrotalcite Mg/Al catalyst for biodiesel production. The results revealed that the basicity of the samples decreased considerably after reuse [98].

ICP-AES is used to evaluate the leaching of metal active phase of the catalyst. Taufiq-Yap et al. reported that the concentration of metal active phase in the solid catalyst was determined and found to be aligned with the obtained of FAME yield [99]. Lee et al. determined Ca, Mg, and Zn content from the catalyst by ICP-AES. It was showed that the only minor of Ca, Mg, and Zn was leached out during reaction and the catalytic activity was still high even after three times use [66].

1.2.5 Regeneration method of solid catalyst

A solid catalyst ideally can be reused many times without any additional treatment. However, deactivation of a used catalyst in transesterification reaction is seen by the drop in the FAME yield [84]. The reusability of a catalyst could be conducted by an additional treatment for regeneration before next use. Generally, after a reaction, the catalyst can be recovered by two major steps: separation from the reaction mixture, and treatment for its regeneration. The solid catalyst generally can be regenerated either by washing, drying, calcination or the combination among them. **Fig. 1.9** illustrates general methods of catalyst regeneration in biodiesel production.

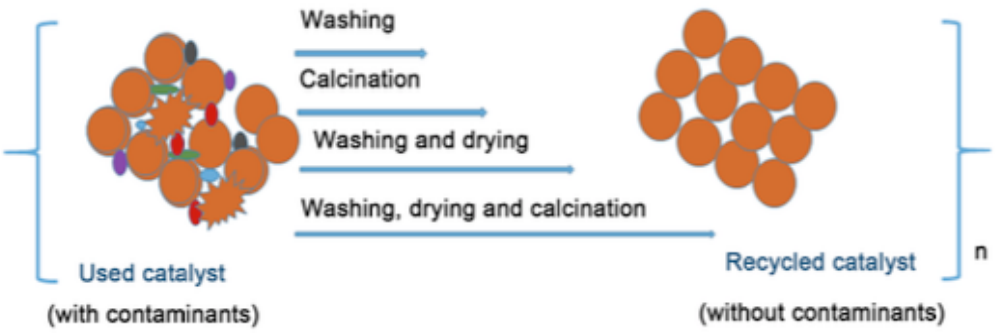

Fig. 1.9. Regeneration methods of solid catalyst [84]

1.3 Alumina industry in Indonesia

Indonesia is one of the bauxite producer country in the world. From 2008 to 2011, bauxite production in Indonesia was increasing rapidly from 8 to 40 million tonnes (**Fig. 1.10**) [100]. In the same time, the industry of bauxite processing for alumina production was started to build. The production capacity of this plant is 300,000 tonnes of alumina per year, it means this country will obtain around 600,000 tonnes of red mud every year [101]. Therefore, the study about red mud utilization should be prepared in order to avoid environmental damage.

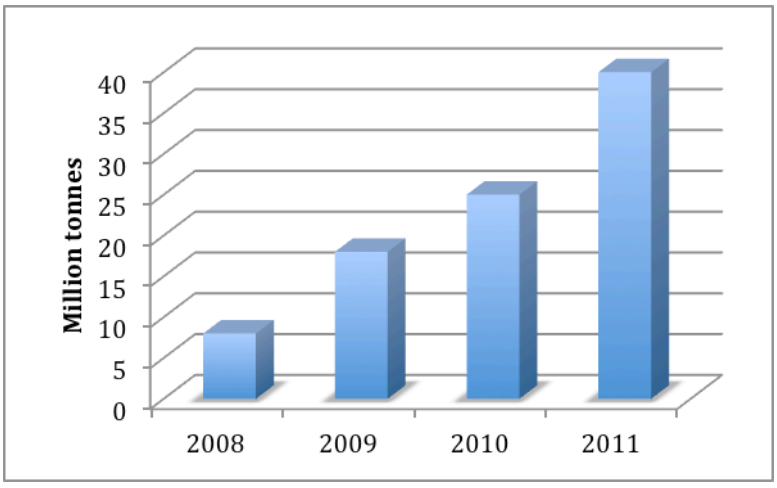

Fig. 1.10. Indonesia bauxite production [100]

1.3.1 Research on red mud utilization in Indonesia

In order to increase the added value of this waste, some studies have been conducted using red mud from Indonesia, such as for geopolymer materials, recovery of iron oxide, and soil remediation.

a) Preparation of geopolymer

Geopolymer is a framework structure produced by condensation of tetrahedral alumino-silicate units, with alkali metal ions balancing the charge associated with tetrahedral Al. Generally, geopolymer is synthesized from a two-part mix, consisting of alumino-silicate materials and alkaline solution. The strong alkaline solution is used to break the chain of Al-Si on alumino-silicate materials to initiate a polymerization reaction via long-range covalent bonds. Thus, geopolymer structure produces dense amorphous phase consisting of semi-crystalline 3-D alumino-silicate microstructure [102,103].

Aziz and Azhari [104] conducted research on utilization of Indonesian red mud for geopolymer material. The objective of this research was to prepare geopolymer by utilizing some wastes, including red mud, to meet the Indonesian National Standard (SNI) of light construction material for housing.

Geopolymer material was prepared by mixing 35% of red mud, 25% of fly ash and 40% of tailing of washed bauxite. The particle distribution of washed bauxite tailing was varied into -12 +16 mesh (25%), -16 +20 mesh (25%), -20 +60 mesh (25%), and -60 +100 mesh (25%), to make the structure more compact. The mixed materials were then added with water and certain amount of sodium silicate (0.5-4% wt) as an activator. Fly ash was obtained from Asam-asam coal power plant, South

Kalimantan, Indonesia, having chemical composition as follows: 42.2% SiO_2, 10.09% Al_2O_3, 23.4% Fe_2O_3, 10.8% CaO, 9.44% MgO, and some minor constituents.

The paste of mixed materials was then molded in a tube standard specimen using hydraulic pressure and cured at 80ºC for 24 h in oven. The dried sample was then aged for 14 days and tested for compressive strength. **Table 1.4** shows the effect of sodium silicate amount on the compressive strength of the specimen.

Table 1.4. Effect of sodium silicate amount on the compressive strength of the specimen [104]

No	Sodium silicate (wt%)	Compressive strength ($kg.cm^{-2}$)
1	0.5%	84.4
2	1%	97.2
3	2%	120.09
4	4%	161.02

The results have fulfilled the requirement of Indonesian National Standard (SNI, Number 15-2094-2000) for producing solid bricks "group of 50" (50-100 $kg.cm^{-2}$), even only by adding small amount of sodium silicate (0.5-1%). The next investigation was preparation of geopolymer with the same composition and 2% sodium silicate without curing. The compressive strength was 65.23 $kg.cm^{-2}$ and fulfilled the standard. The micro-structure shows capillary texture indicates geopolymer phases were formed (**Fig. 1.11**).

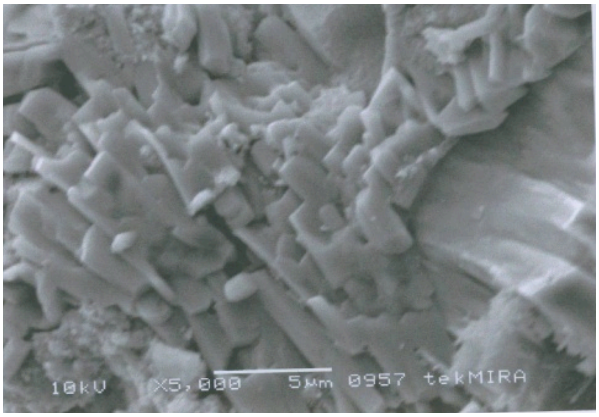

Fig. 1.11. Capillary texture of prepared geopolymer morphology [104]

b) Recovery of iron oxide

Based on the chemical analysis of red mud, iron oxide (Fe_2O_3) is present as a major mineral (more than 30%). Fe_2O_3 is ferromagnetic so it has positive susceptibility on magnetic field. However, the amount of other minerals, such as silica, alumina, and calcite are still high so before conducting magnetic separation, it should be liberated first by scrubbing process in order to optimize on the separation steps.

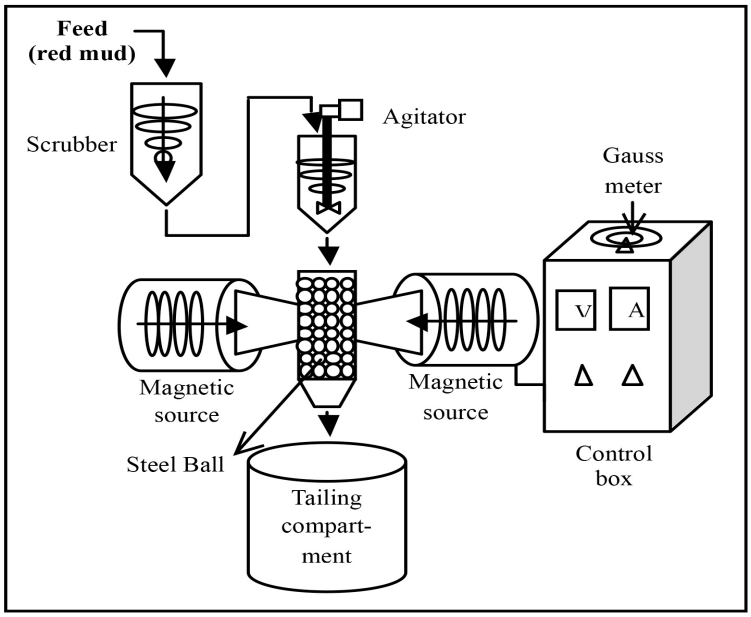

Fig. 1.12. Wet high flux magnetic separator [105]

The recovery of iron oxide from Indonesian red mud was studied by simple method using scrubber and magnetic separator [105]. **Fig. 1.12** shows the separation process of iron oxide mineral. The scrubbing process and magnetic separation were performed in wet condition (10% solid) so that the liberation and separation steps will take place effectively. By adusting the current of electricity or magnetic field strength (Gauss) the magnetic materials would be attracted as concentrate on the induced steel ball while the non-magnetic go through to the tailing compartment.

The effect of magnetic field strength on the recovery of Fe_2O_3 and its content was observed. The measurement was performed from high magnetic field strength to the lower one by repeated cycles. The concentrate obtained from high magnetic field strength was cycled for the next separation at the lower magnetic field. The measurement was performed from 10500 G to 1000 G. The percent recovery of concentrate and Fe_2O_3 content were then observed in every cycle.

Fig. 1.13 shows that high magnetic field strength (10500 G) generated high recovery of concentrate (53.94%) but low content of Fe_2O_3 (50.40%). At high magnetic field strength, the selectivity of attraction of ferro/para-magnetic minerals was low. It means not only ferromagnetic particles will be attracted. The interlocked paramagnetic minerals with gangue minerals would be also attracted to the magnetic field, causing lowering the degree of the purity. After reducing the magnetic field strength gradually up to 1000 G, the recovery was also decreasing (19.59%). Low magnetic field strength only attract the strong ferromagnetic materials (higher selectivity), so the recovery would also decrease, but at the same time, the purity of Fe_2O_3 in concentrate was increasing up to 66.20%.

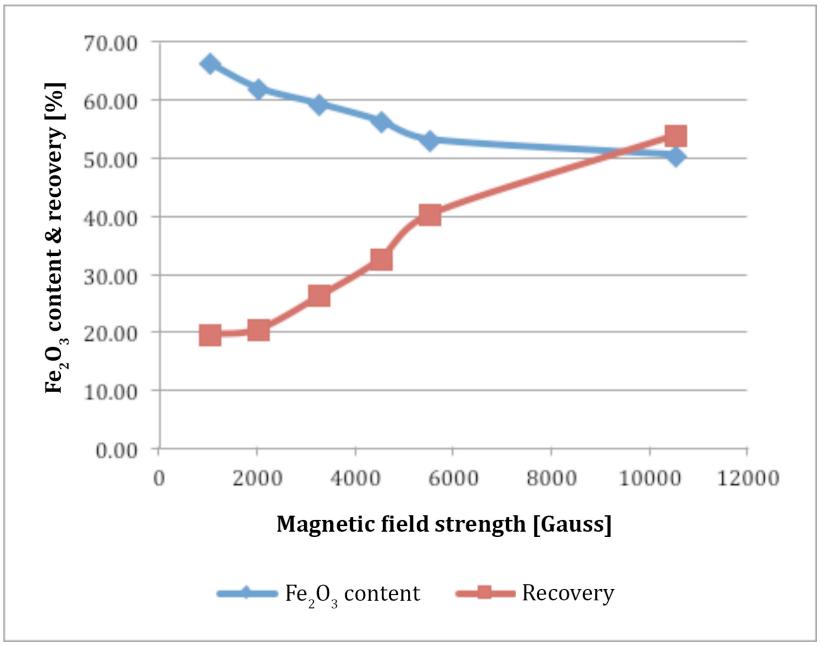

Fig. 1.13. Effect of magnetic field strength on recovery of Fe_2O_3 concentrate and its content [105]

According to this study, iron oxide (Fe_2O_3) can be extracted from red mud by simple two-step process: scrubbing and magnetic separation. To obtain the better result, the additional process should be conducted such as roasting as the first treatment. Roasting can convert hematite (Fe_2O_3) into magnetite (Fe_3O_4). Magnetite has better magnetic susceptibility than hematite so that the recovery by magnetic separation will be more effective.

c) Soil remediation

Purnomo et al. [106] conducted preliminary study of using Indonesian red mud for soil remediation. Most of Kalimantan island is peat area with pH around 3.0-4.5. This situation makes the land unusable for farming and the water not potable due to high acidity. Regarding the high basicity of the Indonesian red mud, it can be potentially utilized as a pH balancer. Besides, peatlands contain large amount of

radical monomers. By applying red mud, which contains iron and aluminum, they might be stabilized by forming complex compounds.

In order to use red mud as soil conditioner, it should pass the environmental risk assessment and effectivenes assessment requirements. The aim of environmental risk assessment is to investigate if the waste is being used or can be used as intended without causing detrimental effects to human health or the environment, such as by toxicity characteristic leaching procedure (TCLP). The effectiveness assessment is conducted after passing the risk assessment. The effectiveness assessment aims to investigate the impact of waste application to the land on plant growth [106].

1.3.2 Potential application of red mud for biodiesel catalyst

In catalysis, red mud has been studied in some applications, such as hydrogenation and liquefaction process [42–44], hydrodechlorination reactions [45,46], and exhaust gas clean up [47]. Aside from that, by utilizing the base property of this waste, it is possible to use it as a base catalyst for biodiesel production. Transesterification process in biodiesel production needs a base catalyst for deprotonating alcohol to convert it into alkoxide. Alkoxide is a strong nucleophile so it can easily react with triglyceride to produce methyl esters as the main product and glycerol as a by product [66]. However, as a waste material, red mud contains high mineral constituents and can act as poison in catalytic reaction.

Application of red mud as solid catalyst for biodiesel production is another promising way to utilize this waste. Although only small amount of red mud is needed (compared to all red mud generated from the process), but it can have an value to be used for energy production. Further, Indonesian government implements mandatory of B20, it means all diesel fuel should be mixed with biodiesel up to 20% [107]. The

increase of biodiesel demand can be supported by providing low cost material for its catalyst. **Fig. 1.14** shows the mandatory of B20 which has started to be implemented by Indonesian government since 2016.

Fig. 1.14. Mandatory of B20 is implemented by Indonesian government [107]

1.4 Modification of red mud

In order to increase the performance of red mud, a pre-treatment or modification of its properties is needed. The modification of red mud can be conducted by several methods, such as acid treatment [108], calcination [2], and soda-lime sintering [109]. By acid treatment, we can separate some metals from the waste, such as iron, and at the same time we can decrease the pH up to neutral pH [108]. Unfortunately, this method is not applicable for biodiesel catalyst, since we need base properties for this purpose.

Calcination has potential impact for red mud modification. The calcined red mud has different properties from the original one due to phase transition during the heat treatment. At 300-550°C, gibbsite decomposes into alumina; while at 600-800°C, calcite decomposes into calcium oxide [2]. The previous study reported that red mud potentially to be used as a basic catalyst for biodiesel production [110]. The calcined red mud was tested for its catalytic activity in several reaction conditions. However,

the highest yield of biodiesel using this catalyst was still lower than the standard specification, although a high amount of methanol had been used (24:1 methanol/oil molar ratio). The EN14214 standard stated that the product should meet the minimum biodiesel yield of 96.5% [111].

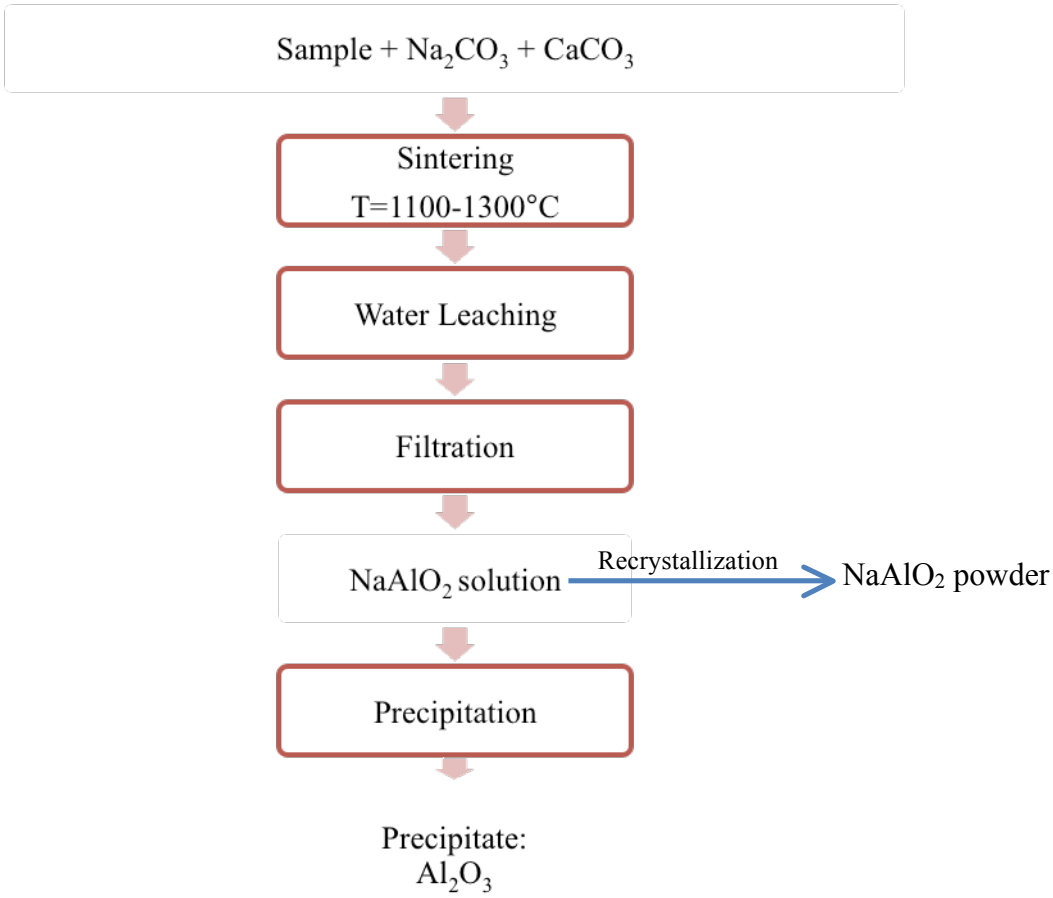

Fig. 1.15. Soda-lime sintering process (adapted from Padilla and Sohn [109])

Soda-lime sintering is another method to treat red mud before applied. This method usually used to extract alumina from materials that contain alumina and silica, such as clay, coal fly ash, and red mud [109]. **Fig. 1.15** shows soda-lime sinter used for extracting alumina from the sample using soda (Na_2CO_3) and limestone ($CaCO_3$) in certain molar ratio. If we notice, sodium aluminate ($NaAlO_2$) solution is produced

as an intermediate product. Sodium aluminate is a compound that have high basicity and high efficiency for biodiesel production [77]. However, the whole process needs high temperature and requires many steps, especially if we intend to recrystallize sodium aluminate solution into powder form.

In this work, we propose to simplify this process by reducing the temperature and shortening the steps, namely soda-lime calcination. The calcined mixture of red mud, Na_2CO_3, and $CaCO_3$ in certain molar ratio is then applied directly as a solid base catalyst for biodiesel production.

1.5 Objectives

The general aim of this research is to utilize red mud, a waste material from alumina industry, as a solid base catalyst for biodiesel production. The following are the specific objectives of this research:

- To prepare a heterogeneous base catalyst from red mud through soda-lime calcination
- To characterize its properties (crystalinity, morphology, basicity, specific surface area)
- To evaluate its catalytic activity for transesterification of canola oil
- To investigate the deactivation factors and the methods to regenerate the activity

1.6 Structure

This dissertation is composed of 5 chapters, and brief description of each chapter is given as follows:

Chapter 1: This chapter provides a background of problem in alumina industry waste, namely red mud, and the potential utilization of this waste into catalyst for biodiesel production. Literature review, potential improvements of red mud, and the objectives of this study are presented in this chapter.

Chapter 2: The modification of Indonesian red mud into solid base catalyst was conducted using soda-lime calcination. The effect of calcination temperature on physical and chemical properties of the catalyst such as crystallinity, morphology, specific surface area, thermogravimetry behavior, and basicity are presented in this chapter.

Chapter 3: The catalytic activity of red mud modified by soda-lime calcination used as a solid base catalyst for transesterification of canola oil was presented in this chapter. The effects of the methanol/oil molar ratio, catalyst amount, reaction temperature, and reaction time were studied to obtain the optimum reaction conditions. Comparison study using different solid base catalyst is also reported in this chapter.

Chapter 4: The deactivation of modified red mud catalyst was studied to obtain the factor(s) that responsible to degradation of its properties and activities. The regeneration of the deactivated catalyst was conducted by calcination, washing with hexane, and combination of them to show the effective method to recover its catalytic activity. The activity of the deactivated and regenerated catalyst were tested in the transesterification of canola oil. The physical and chemical properties of the catalysts such as thermogravimetry behaviour, crystallinity, morphology, specific surface area, and basic strength are also presented in this chapter.

Chapter 5: This chapter presents the general conclusions derived from this research.

References:

[1] P. Wang, D. Liu, Physical and Chemical Properties of Sintering Red Mud and Bayer Red Mud and the Implications for Beneficial Utilization, Materials. 5 (2012) 1800–1810.

[2] C. Wu, D. Liu, Mineral Phase and Physical Properties of Red Mud Calcined at Different Temperatures, Journal of Nanomaterials. 2012 (2012) 1-6.

[3] Red mud production, available online: http://redmud.org/red-mud/production/ (accessed June 12, 2017).

[4] S. Sushil, V.S. Batra, Catalytic applications of red mud, an aluminium industry waste: A review, Applied Catalysis B: Environmental. 81 (2008) 64–77.

[5] E. Balomenos, D. Panias, I. Paspaliaris, Energy and Exergy Analysis of the Primary Aluminum Production Processes : A Review on Current and Future Sustainability, Mineral Processing and Extractive Metallurgy Review. 32 (2011) 68–89.

[6] A. Bhatnagar, V.J.P. Vilar, C.M.S. Botelho, R.A.R. Boaventura, A review of the use of red mud as adsorbent for the removal of toxic pollutants from water and wastewater, Environmental Technology. 32 (2011) 231–249.

[7] P. Renforth, W.M. Mayes, A.P. Jarvis, I.T. Burke, D.A.C. Manning, K. Gruiz, Contaminant mobility and carbon sequestration downstream of the Ajka (Hungary) red mud spill: The effects of gypsum dosing, Science of the Total Environment. 421–422 (2012) 253–259.

[8] Commission Decision 2000/532/EC, OJ L 226, 06.09.2000, 3–24. available online: http://eur-lex.europa.eu/legal-content/EN/TXT/PDF/?uri=CELEX:22002D0009&from=EN (accessed June 7, 2017).

[9] S. Wang, H.M. Ang, M.O. Tadé, Novel applications of red mud as coagulant, adsorbent and catalyst for environmentally benign processes, Chemosphere. 72 (2008) 1621–1635.

[10] Red mud disposal, available online: http://redmud.org/red-mud/disposal/ (accessed June 12, 2017).

[11] J. Hyun, S. Endoh, K. Masuda, Reduction of chlorine in bauxite residue by fine particle separation, International Journal of Mineral Processing. 76 (2005) 13–20.

[12] Red mud, available online: https://en.wikipedia.org/wiki/Red_mud (accessed June 12, 2017).

[13] Red mud in Hungary, available online: https://aboutenvironment.wordpress.com/2010/10/07/red-mud-in-hungary/ (accessed June 7, 2017).

[14] S. Wang, Y. Boyjoo, A. Choueib, Z.H. Zhu, Removal of dyes from aqueous solution using fly ash and red mud, Water Research. 39 (2005) 129–138.

[15] C. Brunori, C. Cremisini, P. Massanisso, V. Pinto, L. Torricelli, Reuse of a treated red mud bauxite waste: studies on environmental compatibility, Journal of Hazardous Materials. 117 (2005) 55–63.

[16] M. Singhl, S.N. Upadhayay, P.M. Prasad, Preparation of iron rich cements using red mud, Cement and Conrete Research. 27 (1997) 1037–1046.

[17] Red mud characteristics, available online: http://redmud.org/red-mud/characteristics/ (accessed June 12, 2017).

[18] S. Samal, A.K. Ray, A. Bandopadhyay, Proposal for resources , utilization and processes of red mud in India — A review, International Journal of Mineral Processing. 118 (2013) 43–55.

[19] É. Ujaczki, Y.S. Zimmermann, C.A. Gasser, M. Molnár, M. Lenz, Red mud as secondary source for critical raw materials – extraction study, Journal of Chemical Technology and Biotechnology. (2017) 1–10.

[20] A.P. Yang, The development of brick made of red mud and fly ash, Light Metals. 12 (1996) 17–18.

[21] S. Rai, D.H. Lataye, M.J. Chaddha, R.S. Mishra, P. Mahendiran, J.

Mukhopadhyay, C. Yoo, K.L. Wasewar, An Alternative to Clay in Building Materials : Red Mud Sintering Using Fly Ash via Taguchi ' s Methodology, Advances inMaterials Science and Engineering. 2013 (2013) 1–7.

[22] E. Kalkan, Utilization of red mud as a stabilization material for the preparation of clay liners, Engineering Geology. 87 (2006) 220–229.

[23] I. Vangelatos, G.N. Angelopoulos, D. Boufounos, Utilization of ferroalumina as raw material in the production of Ordinary Portland Cement, Journal of Hazardous Materials. 168 (2009) 473–478.

[24] N. Yalçın, V. Sevinç, Utilization of bauxite waste in ceramic glazes, Ceramics International. 26 (2000) 485–493.

[25] F. Peng, K. Liang, A. Hu, H. Shao, Nano-crystal glass-ceramics obtained by crystallization of vitrified coal fly ash, Chemosphere. 59 (2005) 899–903.

[26] Y. Pontikes, P. Nikolopoulos, G.N. Angelopoulos, Thermal behaviour of clay mixtures with bauxite residue for the production of heavy-clay ceramics, Journal of the European Ceramic Society. 27 (2007) 1645–1649.

[27] A. Tor, Y. Cengeloglu, M.E. Aydin, M. Ersoz, Removal of phenol from aqueous phase by using neutralized red mud, Journal of Colloid and Interface Science. 300 (2006) 498–503.

[28] M. Vaclavikova, P. Misaelides, G. Gallios, S. Jakabsky, S. Hredzak, Removal of cadmium, zinc, copper and lead by red mud, an iron oxides containing hydrometallurgical waste, Studies in Surface Science and Catalysis. 155 (2005) 517–525.

[29] M. Erdem, H.S. Altundoğan, F. Tümen, Removal of hexavalent chromium by using heat-activated bauxite, Minerals Engineering. 17 (2004) 1045–1052.

[30] L. Santona, P. Castaldi, P. Melis, Evaluation of the interaction mechanisms between red muds and heavy metals, Journal of Hazardous Materials. 136 (2006) 324–329.

[31] Y. Cengeloglu, A. Tor, M. Ersoz, G. Arslan, Removal of nitrate from aqueous

solution by using red mud, Separation and Purification Technology. 51 (2006) 374–378.

[32] G. Akay, B. Keskinler, A. Cakici, U. Danis, Phosphate removal from water by red mud using crossflow microfiltration, Water Research. 32 (1998) 717–726.

[33] S. Wang, Y. Boyjoo, A. Choueib, Z.H. Zhu, Removal of dyes from aqueous solution using fly ash and red mud, Water Research. 39 (2005) 129–138.

[34] I. Ghosh, S. Guha, R. Balasubramaniam, A.V.R. Kumar, Leaching of metals from fresh and sintered red mud, Journal of Hazardous Materials. 185 (2011) 662–668.

[35] S. Rai, K.L. Wasewar, J. Mukhopadhyay, C.K. Yoo, H. Uslu, Neutralization and utilization of red mud for its better waste management, Arch. Environ. Sci. 6 (2012) 13–33.

[36] X.F. Zheng, Recycling technology of aluminum and sodium from low temperature bayer progress red mud, Shandong Metall. 32 (2010) 16–17.

[37] L. Zhong, Y.F. Zhang, Sub molten salt method recycling red mud, Chin. J. Nonferrous Met. 18 (2008) 70–73.

[38] Y.F. Sun, F.Z. Dong, J.T. Liu, S. WANG, Technology for recovering iron from red mud by Bayer process, Metal Mine. 9 (2009) 176–178.

[39] D.I. Smirnov, T. V Molchanova, The investigation of sulphuric acid sorption recovery of scandium and uranium from the red mud of alumina production, Hydrometallurgy. 45 (1997) 249–259.

[40] X.H. Chen, Y. Chen, M. Gan, K.X. Xu, Precipitation and separation of vanadium from bayer process sodium aluminate solution, The Chinese Journal of Process Engineering. 10 (2010) 24–38.

[41] M. Ochsenkühn-Petropulu, T. Lyberopulu, G. Parissakis, Selective separation and determination of scandium from yttrium and lanthanides in red mud by a combined ion exchange/solvent extraction method, Analytica Chimica Acta. 315 (1995) 231–237.

[42] A.M. Mastral, C. Mayoral, M.T. Izquierdo, C. Pardos, Iron catalyzed hydrogenation of high sulphur content coals, Fuel Processing Technology. 36 (1993) 177–184.

[43] S. Yokoyama, M. Yamamoto, Y. Maekawa, T. Kotanigawa, Catalytic activity of sulphate for hydroliquefaction of coal by using diphenylether and diphenylmethane, Fuel. 68 (1989) 531–533.

[44] B. Klopries, W. Hodek, F. Bandermann, Catalytic hydroliquefaction of biomass with red mud and cobalt monoxide-molybdenum trioxide catalysts., Fuel. 69 (1990) 448–455.

[45] J. Halász, M. Hodos, I. Hannus, G. Tasi, I. Kiricsi, Catalytic detoxification of C2-chlorohydrocarbons over iron-containing oxide and zeolite catalysts, Colloids and Surfaces A: Physicochemical and Engineering Aspects. 265 (2005) 171–177.

[46] S. Ordóez, H. Sastre, F. V. Díez, Catalytic hydrodechlorination of tetrachloroethylene over red mud, Journal of Hazardous Materials. 81 (2001) 103–114.

[47] J.R. Paredes, S. Ordóñez, A. Vega, F. V. Díez, Catalytic combustion of methane over red mud-based catalysts, Applied Catalysis B: Environmental. 47 (2004) 37–45.

[48] M.S. Rukhlyadeva, M. V Belousov, E.A. Nikonenko, G. V Ismagilova, M.P. Kolesnikova, Production of black iron oxide from red mud, Russian Journal of Applied Chemistry. 88 (2015) 377–381.

[49] N. Yamada, H. Hirosue, Utilization of Red Mud as a Red-colored Pigment and Its Characteristics, Journal of the Society of Powder Technology, Japan. 18 (1981) 760–768.

[50] J. Pera, R. Boumaza, J. Ambroise, Development of a pozzolanic pigment from red mud, Cement and Concrete Research. 27 (1997) 1513–1522.

[51] C.W. Gray, S.J. Dunham, P.G. Dennis, F.J. Zhao, S.P. McGrath, Field

evaluation of in situ remediation of a heavy metal contaminated soil using lime and red-mud, Environmental Pollution. 142 (2006) 530–539.

[52] A.F. Bertocchi, M. Ghiani, R. Peretti, A. Zucca, Red mud and fly ash for remediation of mine sites contaminated with As, Cd, Cu, Pb and Zn, Journal of Hazardous Materials. 134 (2006) 112–119.

[53] S. Al-Zuhair, Production of biodiesel: possibilities and challenges, Biofuels, Bioproducts and Biorefining. 1 (2007) 57–66.

[54] Z. Helwani, M.R. Othman, N. Aziz, W.J.N. Fernando, J. Kim, Technologies for production of biodiesel focusing on green catalytic techniques: A review, Fuel Processing Technology. 90 (2009) 1502–1514.

[55] F. Guo, Z. Fang, Biodiesel Production with Solid Catalysts, in: M. Stoytcheva (Ed.), Biodiesel Feedstocks and Processing Technologies, In Tech, Rijeka, 2011: pp. 339–358.

[56] G. Mushrush, E.J. Beal, G. Spencer, J.H. Wynne, C.L. Lloyd, J.M. Hughes, C.L. Walls, D.R. Hardy, G. Mushrush, E.J. Beal, G. Spencer, J.H. Wynne, C.L. Lloyd, J.M. Hughes, C.L. Walls, D.R.H. An, An environmentally benign soybean derived fuel as a blending stock or replacement for home heating oil, Journal of Environmental Science and Health, Part A. 36 (2001) 613–622.

[57] D.A. Wardle, Global sale of green air travel supported using, Renewable and Sustainable Energy Reviews. 7 (2003) 1–64.

[58] R. Romero, S.L. Martínez, R. Natividad, Biodiesel Production by Using Heterogeneous Catalysts, in: M. Manzanera (Ed.), Alternatif Fuel, In Tech, Rijeka, 2011: pp. 3–20.

[59] A.L. de Lima, C.M. Ronconi, C.J.A. Mota, Heterogeneous basic catalysts for biodiesel production, Catal. Sci. Technol. 6 (2016) 2877–2891.

[60] D.E. López, J.G. Goodwin, D.A. Bruce, E. Lotero, Transesterification of triacetin with methanol on solid acid and base catalysts, Applied Catalysis A: General. 295 (2005) 97–105.

[61] C.O. Pereira, M.F. Portilho, C.A. Henriques, F.M.Z. Zotin, SnSO4 as catalyst for simultaneous transesterification and esterification of acid soybean oil, Journal of the Brazilian Chemical Society. 25 (2014) 2409–2416.

[62] J.M. Encinar, J.F. Gonzalez, A. Rodriguez-Reinares, Biodiesel from used frying oil. Variables affecting the yields and characteristics of the biodiesel, Industrial and Engineering Chemistry Research. 44 (2005) 5491–5499.

[63] M. Verziu, S.M. Coman, R. Richards, V.I. Parvulescu, Transesterification of vegetable oils over CaO catalysts, Catalysis Today. 167 (2011) 64–70.

[64] A. Demirbas, Biodiesel production from vegetable oils by supercritical methanol, Journal of Scientific & Industrial Research. 64 (2005) 858–865.

[65] P.M. Ejikeme, I.D. Anyaogu, C.L. Ejikeme, N.P. Nwafor, C.A.C. Egbuonu, K. Ukogu, J.A. Ibemesi, I. Chemistry, F. Polytechnic, Catalysis in Biodiesel Production by Transesterification Process-An Insight, E-Journal of Chemistry. 7 (2010) 1120–1132.

[66] H. V Lee, J.C. Juan, N.F. Binti Abdullah, R. Nizah Mf, Y.H. Taufiq-Yap, Heterogeneous base catalysts for edible palm and non- edible Jatropha- based biodiesel production, Chemistry Central Journal. 8 (2014) 1–9.

[67] Transesterification, available online: https://en.wikipedia.org/wiki/ Transesterification (accessed June 12, 2017).

[68] H. Fukuda, A. Kondo, H. Noda, Biodiesel fuel production by transesterification of oils, Journal of Bioscience and Bioengineering. 92 (2001) 405–416. doi:10.1016/S1389-1723(01)80288-7.

[69] G. Arzamendi, I. Campo, E. Arguiñarena, M. Sánchez, M. Montes, L.M. Gandía, Synthesis of biodiesel with heterogeneous NaOH/alumina catalysts: Comparison with homogeneous NaOH, Chemical Engineering Journal. 134 (2007) 123–130.

[70] K.G. Georgogianni, A.K. Katsoulidis, P.J. Pomonis, G. Manos, M.G. Kontominas, Transesterification of rapeseed oil for the production of biodiesel

using homogeneous and heterogeneous catalysis, Fuel Processing Technology. 90 (2009) 1016–1022.

[71] M. Zabeti, W.M.A. Wan Daud, M.K. Aroua, Activity of solid catalysts for biodiesel production: A review, Fuel Processing Technology. 90 (2009) 770–777.

[72] A.F. Lee, J. a Bennett, J.C. Manayil, K. Wilson, Heterogeneous catalysis for sustainable biodiesel production via esterification and transesterification., Chemical Society Reviews. 43 (2014) 7887–7916.

[73] S. Semwal, A.K. Arora, R.P. Badoni, D.K. Tuli, Biodiesel production using heterogeneous catalysts, Bioresource Technology. 102 (2011) 2151–2161.

[74] T.F. Dossin, M.F. Reyniers, R.J. Berger, G.B. Marin, Simulation of heterogeneously MgO-catalyzed transesterification for fine-chemical and biodiesel industrial production, Applied Catalysis B: Environmental. 67 (2006) 136–148.

[75] A. Kawashima, K. Matsubara, K. Honda, Acceleration of catalytic activity of calcium oxide for biodiesel production, Bioresource Technology. 100 (2009) 696–700.

[76] S. Gryglewicz, Rapeseed oil methyl esters preparation using heterogeneous catalysts, Bioresource Technology. 70 (1999) 249-253.

[77] T. Wan, P. Yu, S. Wang, Y. Luo, Application of sodium aluminate as a heterogeneous base catalyst for biodiesel production from soybean oil, Energy and Fuels. 23 (2009) 1089–1092.

[78] F. Guo, Z.G. Peng, J.Y. Dai, Z.L. Xiu, Calcined sodium silicate as solid base catalyst for biodiesel production, Fuel Processing Technology. 91 (2010) 322–328.

[79] S.K. Cherikkallinmel, A. Gopalakrishnan, Z. Yaakob, R.M. Ramakrishnan, S. Sugunan, B.N. Narayanan, Sodium aluminate from waste aluminium source as catalyst for the transesterification of Jatropha oil, RSC Adv. 5 (2015) 46290–

46294.

[80] S. Ismail, a. S. Ahmed, R. Anr, S. Hamdan, Biodiesel Production from Castor Oil by Using Calcium Oxide Derived from Mud Clam Shell, Journal of Renewable Energy. 2016 (2016) 1–8.

[81] B. Aghabarari, M. V. Martinez-Huerta, Biodiesel Production Using Calcined Waste Filter Press Cake from a Sugar Manufacturing Facility as a Highly Economic Catalyst, Journal of the American Oil Chemists' Society. 93 (2016) 773–779.

[82] V. Vadery, B.N. Narayanan, R.M. Ramakrishnan, S.K. Cherikkallinmel, S. Sugunan, D.P. Narayanan, S. Sasidharan, Room temperature production of jatropha biodiesel over coconut husk ash, Energy. 70 (2014) 588–594.

[83] M. Argyle, C. Bartholomew, Heterogeneous Catalyst Deactivation and Regeneration: A Review, Catalysts. 5 (2015) 145–269.

[84] N. Oueda, Y.L. Bonzi-Coulibaly, I.W.K. Ouédraogo, Deactivation Processes, Regeneration Conditions and Reusability Performance of CaO or MgO Based Catalysts Used for Biodiesel Production—A Review, Materials Sciences and Applications. 8 (2017) 94–122.

[85] M. Kouzu, T. Kasuno, M. Tajika, Y. Sugimoto, S. Yamanaka, J. Hidaka, Calcium oxide as a solid base catalyst for transesterification of soybean oil and its application to biodiesel production, Fuel. 87 (2008) 2798–2806.

[86] A. Singh, B. He, J. Thompson, J. Van Gerpen, Process optimization of biodiesel production using alkaline catalysts, Applied Engineering in Agriculture. 22 (2006) 597–600.

[87] S. Xia, X. Guo, D. Mao, Z. Shi, G. Wu, G. Lu, Biodiesel synthesis over the CaO–ZrO 2 solid base catalyst prepared by a urea–nitrate combustion method, RSC Adv. 4 (2014) 51688–51695.

[88] H.N. Pham, J. Reardon, A.K. Datye, Measuring the strength of slurry phase heterogeneous catalysts, Powder Technology. 103 (1999) 95–102.

[89] P. Nair, B. Singh, S.N. Upadhyay, Y.C. Sharma, Synthesis of biodiesel from low FFA waste frying oil using calcium oxide derived from Mereterix mereterix as a heterogeneous catalyst, Journal of Cleaner Production. 29 (2012) 82–90.

[90] B. Wang, S. Li, S. Tian, R. Feng, Y. Meng, A new solid base catalyst for the transesterification of rapeseed oil to biodiesel with methanol, Fuel. 104 (2013) 698–703.

[91] M. Liu, S. Niu, C. Lu, S. Cheng, An optimization study on transesterification catalyzed by the activated carbide slag through the response surface methodology, Energy Conversion and Management. 92 (2015) 498–506.

[92] F.J. Li, H.Q. Li, L.G. Wang, Y. Cao, Waste carbide slag as a solid base catalyst for effective synthesis of biodiesel via transesterification of soybean oil with methanol, Fuel Processing Technology. 131 (2015) 421–429.

[93] X. Deng, Z. Fang, Y. hu Liu, C.L. Yu, Production of biodiesel from Jatropha oil catalyzed by nanosized solid basic catalyst, Energy. 36 (2011) 777–784.

[94] W.W.S. Ho, H.K. Ng, S. Gan, S.H. Tan, Evaluation of palm oil mill fly ash supported calcium oxide as a heterogeneous base catalyst in biodiesel synthesis from crude palm oil, Energy Conversion and Management. 88 (2014) 1167–1178.

[95] Z. Wen, X. Yu, S.-T. Tu, J. Yan, E. Dahlquist, Biodiesel production from waste cooking oil catalyzed by TiO2-MgO mixed oxides, Bioresource Technology. 101 (2010) 9570–9576.

[96] M. Kaur, A. Ali, Ethanolysis of waste cottonseed oil over lithium impregnated calcium oxide: Kinetics and reusability studies, Renewable Energy. 63 (2014) 272–279.

[97] A.A. Refaat, Biodiesel production using solid metal oxide catalysts, International Journal of Environmental Science & Technology. 8 (2011) 203–221.

[98] C.C.C.M. Silva, N.F.P. Ribeiro, M.M.V.M. Souza, D.A.G. Aranda, Biodiesel production from soybean oil and methanol using hydrotalcites as catalyst, Fuel Processing Technology. 91 (2010) 205–210.

[99] Y.H. Taufiq-Yap, S.H. Teo, U. Rashid, A. Islam, M.Z. Hussien, K.T. Lee, Transesterification of Jatropha curcas crude oil to biodiesel on calcium lanthanum mixed oxide catalyst: Effect of stoichiometric composition, Energy Conversion and Management. 88 (2014) 1290–1296.

[100] Ministry of Energy and Mineral Resources, Indonesia, Affect of bauxite processing on economic value of West Kalimantan region, available online: https://www.esdm.go.id/assets/media/content/content-dampak-hilirisasi-mineral-bauksit-terhadap-perekonomian-provinsi-kalimantan-barat.pdf (accessed June 7, 2017).

[101] Ministry of Energy and Mineral Resources, Indonesia, Study on policy of mineral industry development, available online: http://prokum.esdm.go.id /Publikasi/Hasil Kajian/ESDM KEK.pdf (accessed June 7, 2017).

[102] D. Feng, J.L. Provis, J.S.J. van Deventer, Thermal Activation of Albite for the Synthesis of One-Part Mix Geopolymers, Journal of the American Ceramic Society. 95 (2012) 565–572.

[103] K. Pimraksa, P. Chindaprasirt, A. Rungchet, K. Sagoe-Crentsil, T. Sato, Lightweight geopolymer made of highly porous siliceous materials with various Na2O/Al2O3 and SiO2/Al2O3 ratios, Materials Science and Engineering: A. 528 (2011) 6616–6623.

[104] M. Aziz, Azhari, Preparation of red mud-based geopolymer for building materials, Journal of Mineral and Coal Technology. 10 (2014) 32–43.

[105] A. Wahyudi, A. Yudhistira, M. Aziz, D. Amalia, A. Sudarsono, Preliminary Study of Extraction Iron Oxide Concentrate from Red Mud Using Scrubbing Method and Magnetic Separator, in: Proceedings International Conference on Materials and Metallurgical Technology, Surabaya, 2009.

[106] H. Purnomo, T. Wahyudi, M. Aziz, Husaini, B. Agung, T. Soenara, Jafril, H.

Hariyadi, A. Wahyudi, R. Iriansyah, Report: Study on acceleration technology of bauxite upgrading and red mud utilization in Indonesia, R&D Centre of Mineral and Coal Technology, Bandung, 2014.

[107] I. Paryanto, Indonesian policy toward high blend of biodiesel for transportation and market experince, in: Workshop on Higher Blending of Biodiesel Utilization in ASEAN, Bangkok, 2015: pp. 17–18.

[108] S. Sushil, V.S. Batra, Modification of red mud by acid treatment and its application for CO removal, Journal of Hazardous Materials. 203–204 (2012) 264–273.

[109] R. Padilla, H.Y. Sohn, Sodium aluminate leaching and desilication in lime-soda sinter process for alumina from coal wastes, Metallurgical Transactions B. 16 (1985) 707–713.

[110] Q. Liu, R. Xin, C. Li, C. Xu, J. Yang, Application of red mud as a basic catalyst for biodiesel production, Journal of Environmental Sciences. 25 (2013) 823–829.

[111] I. Barabás, I.-A. Todorut, Biodiesel Quality, Standards and Properties, in: G. Montero (Ed.), Biodiesel: Quality, Emissions and by-Products, In Tech, Rijeka, 2011: pp. 3–28.

Chapter 2

Synthesis of Solid Base Catalyst from Red Mud Using Soda-lime Calcination

The modification of Indonesian red mud into solid base catalyst was conducted using soda-lime calcination. The effect of calcination temperature on physical and chemical properties of the catalyst such as crystallinity, morphology, specific surface area, thermogravimetry behavior, and basicity are presented in this chapter.

2.1 Catalyst preparation

The catalysts were prepared by modification of red mud through soda-lime calcination (**Fig. 2.1**). Red mud was obtained from the R&D Centre for Mineral and Coal Technology, the Ministry of Energy and Mineral Resources, Indonesia. It was dried at 105°C for 24 h in an oven to remove moisture content from its structure. Sodium carbonate was purchased from Wako Pure Chemical Industries, Ltd. Limestone (calcium carbonate) was obtained from an Indonesia local market with 94% CaO content. The three components were mixed and ground at the molar ratio of Na_2O/Al_2O_3 and CaO/Si_2O_3 of 1.5 and 2, respectively. The mixed components were then sieved to obtain fine material with the particle size of 150 μm and labeled as RSL-uncalcined, where RSL is an abbreviation of the three components: red mud, soda and limestone. Otherwise, the mixed components were calcined at different temperatures (500, 700 and 900°C) for 2 h under air flow, and labeled as RSL-X, where X corresponds to the calcination temperature.

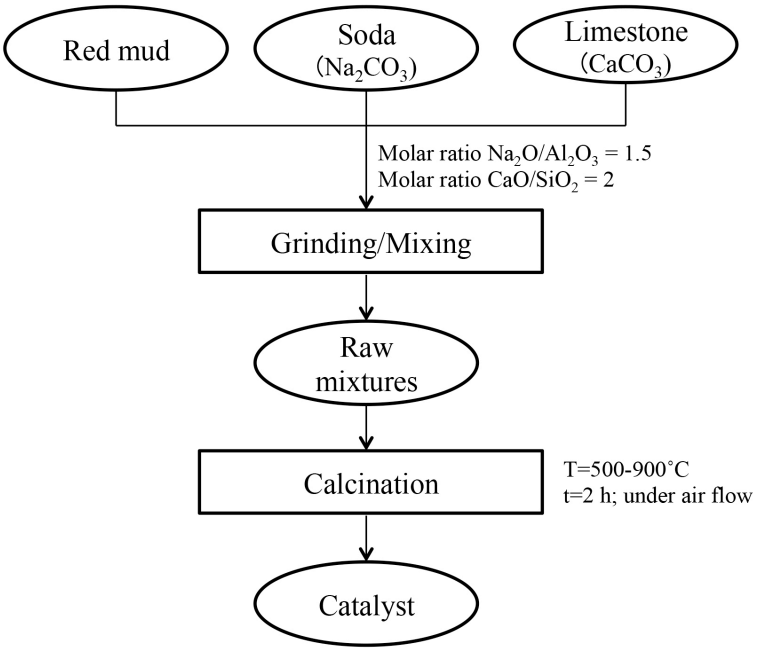

Fig. 2.1. Catalyst preparation from red mud using soda-lime calcination

2.2 Instrumentation

X-ray diffraction (XRD) of the catalysts was conducted for the crystallinity and mineral contents identification. XRD analysis were done using a Rigaku Multiflex X-ray diffractometer with Cu-Kα radiation (λ = 1.54056Å) at 40 kV, 20 mA over the 2-theta range of 15–40°. Thermogravimetry (TG) and differential thermal analysis (DTA) were carried out using a Rigaku Thermoplus TG 8120 under air flow at a heating rate of 10˚C/min up to 900˚C. Morphological observation by scanning electron microscope (SEM) was performed using a Keyence VE-8800. Nitrogen adsorption analysis was conducted to measure the specific surface area of the catalyst (calculated by BET method) using an Autosorb-1C (AX1C-MP-LP Quantachrome Instruments). The elemental composition was determined using inductively coupled plasma atomic emission spectroscopy (ICP-AES, SPS 7800 Seiko Instruments Inc.). The basic strength of prepared catalyst was determined using Hammett indicators [1,2]. The following Hammett indicators were used in these

experiments: bromothymol blue (H_=7.2), phenolphthalein (H_=9.3), 2,4-dinitroaniline (H_=15.0), and 4-chloro-2-nitroaniline (H_=17.2). The basicity of the solid catalyst was measured by the method of Hammett indicator-benzoic acid titration [3].

2.3 Characterization of Indonesian red mud

Fig. 2.2 shows the XRD pattern of red mud. It was found that this waste contains many residual minerals from bauxite, such as hematite (Fe_2O_3), gibbsite ($Al(OH)_3$), calcite ($CaCO_3$), and quartz (SiO_2). Iron oxide and aluminum hydroxide phases were commonly found in the red mud [4]. Chemical analysis reveals that red mud contains Fe, Al, Si, Na, as well as minor constituents, such as Ti, Ca, Mg, Zr and Mn (**Table 2.1**).

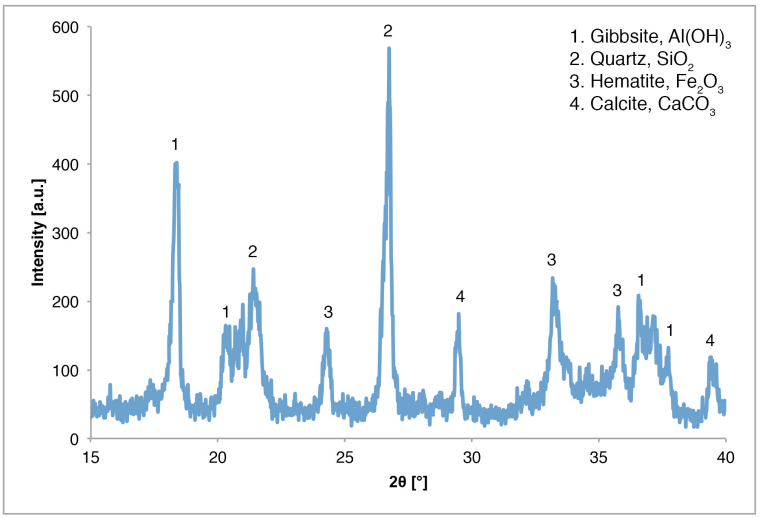

Fig. 2.2. XRD pattern of Indonesian red mud

Table 2.1. Chemical composition of Indonesian red mud

Chemical composition	SiO_2	Al_2O_3	Fe_2O_3	Na_2O	TiO_2	CaO	MgO	ZrO_2	MnO_2	Others
% weight	13.8	24.63	33.36	7.98	1.33	0.57	0.05	0.03	0.05	18.2

2.4 Effect of calcination temperature on physical and chemical properties of the catalyst

Fig. 2.3 shows the catalysts prepared by soda-lime calcination of red mud. The mass of each prepared catalyst tend to decrease with the increase of calcination temperature. The mass percentage of RSL-500, RSL-700, and RSL-900 were 85.06%, 75.29%, and 67.65%, respectively, compared to the uncalcined one. TG-DTA analysis will explain about these results.

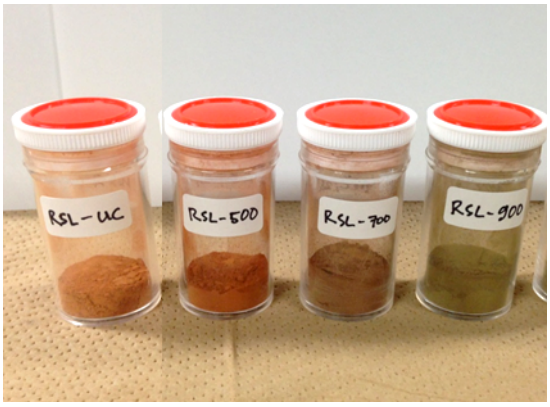

Fig. 2.3. The synthesized catalysts prepared by different calcinaiton temperatures

The TG-DTA profiles of an uncalicined mixture of red mud, sodium carbonate, and limestone are shown in **Fig. 2.4**. The endothermic DTA peaks occured at several ranges and TG curves indicated the mass loss for each transformation. The first three peaks ranged between 40–100°C, 240–300°C and 450–500°C with the mass loss of about 14% were mainly related to the removal of bonded water molecules. The next mass loss of 18% occurring within the interval 650–850°C and 850–900°C corresponding to the elimination of carbon dioxide during the decomposition of carbonates.

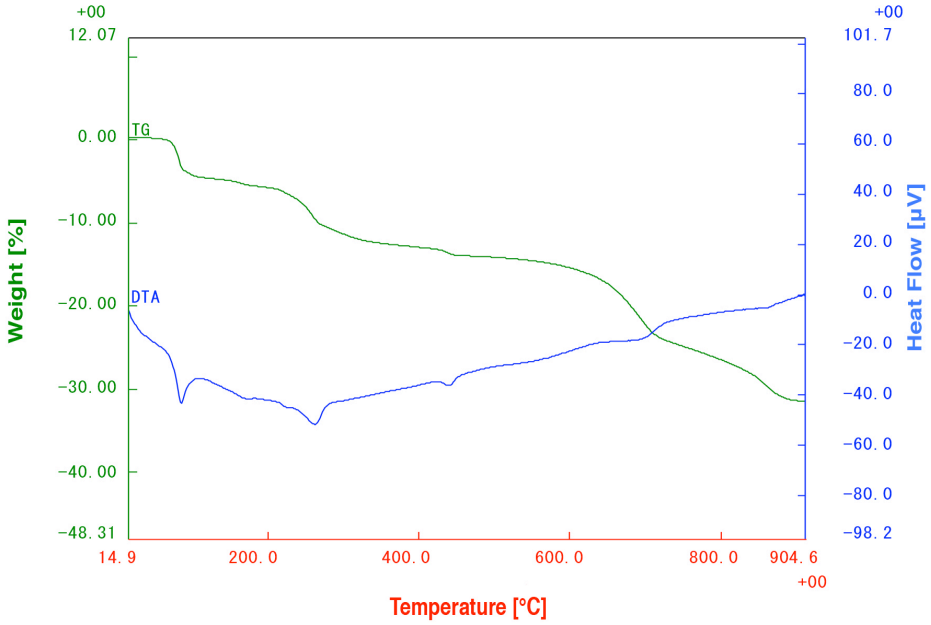

Fig. 2.4. TG-DTA profiles of RSL-uncalcined

The basic property (basic strength and basicity) of each catalyst are summarized in **Table 2.2**. The total basicities of the solid surface of the catalysts tend to increase with increasing calcination temperature.

Table 2.2. Basic properties of synthesized catalysts

Catalyst	Basicity of each basic strength ranges [mmol/g]			
	H_ = 7.2-9.8	H_ = 9.8-15.0	H_ = 15.0-17.2	Total basicity
RSL-uncalcined	1.44	0	0	1.44
RSL-500	1.28	0.32	0.16	1.76
RSL-700	0.76	0.72	0.40	1.88
RSL-900	0.80	1.16	0	1.96

The XRD patterns shown in **Fig. 2.5** reveal the crystallinity and mineral transformation during calcination. The pattern of RSL-uncalcined (**Fig. 2.5a**) labeled with numbers 1 to 7 shows the original mineral contents of the three components of the mixture: red mud, sodium carbonate and limestone. The crystallite

phase transformation from calcium hydroxide to calcium oxide occurring at the temperature greater than 450°C was due to the dehydration reactions, as presented in Eq. (2.1) [5].

$$Ca(OH)_2 \rightarrow CaO + H_2O \quad (2.1)$$

$$CaCO_3 \rightarrow CaO + CO_2 \quad (2.2)$$

The catalyst synthesized at 700°C has higher basicity due to the crytallite phase transformation from calcium carbonate to calcium oxide, as presented in Eq. (2.2) [6]. Besides that, Padilla and Shon (1985a) reported material that contains alumina and silica while heated with sodium carbonate and limestone would form sodium aluminate and calcium silicate. Since red mud also contains alumina and silica, a similar behavior is expected to be exhibited during calcination of the mixtures. The expression for the reaction can be written as presented in Eq. (2.3) [7].

$$Al_2O_3 + 2SiO_2 + Na_2CO_3 + 4CaCO_3 \rightarrow 2NaAlO_2 + 2Ca_2SiO_4 + 5CO_2 \quad (2.3)$$

$$Na_2CO_3 + Al_2O_3 \rightarrow 2NaAlO_2 + CO_2 \quad (2.4)$$

$$Na_2CO_3 + 2SiO_2 \rightarrow Na_2Si_2O_5 + CO_2 \quad (2.5)$$

$$Na_2Si_2O_5 + 4CaCO_3 + Al_2O_3 \rightarrow 2NaAlO_2 + 2Ca_2SiO_4 + 4CO_2 \quad (2.6)$$

$$Na_2CO_3 + 2Al_2O_3 + 3CaCO_3 \rightarrow 2NaAlO_2 + Ca_3Al_2O_6 + 4CO_2 \quad (2.7)$$

$$2NaAlO_2 + SiO_2 \rightarrow Na_2Al_2SiO_6 \quad (2.8)$$

The expression in Eq. (2.3) can be detailed into several reactions as presented in Eqs. (2.4)–(2.6). Sodium silicate and sodium aluminate started to form at that temperature (**Fig. 2.5c**, Nos. 8 and 9). Tao et al. (2009) and Guo et al. (2010) reported

that those materials had high basicity and high efficiency for biodiesel production [8,9]. The increase in temperature and the excess of calcium carbonate made sodium silicate transform into calcium silicate (**Fig. 2.5d**, No. 10).

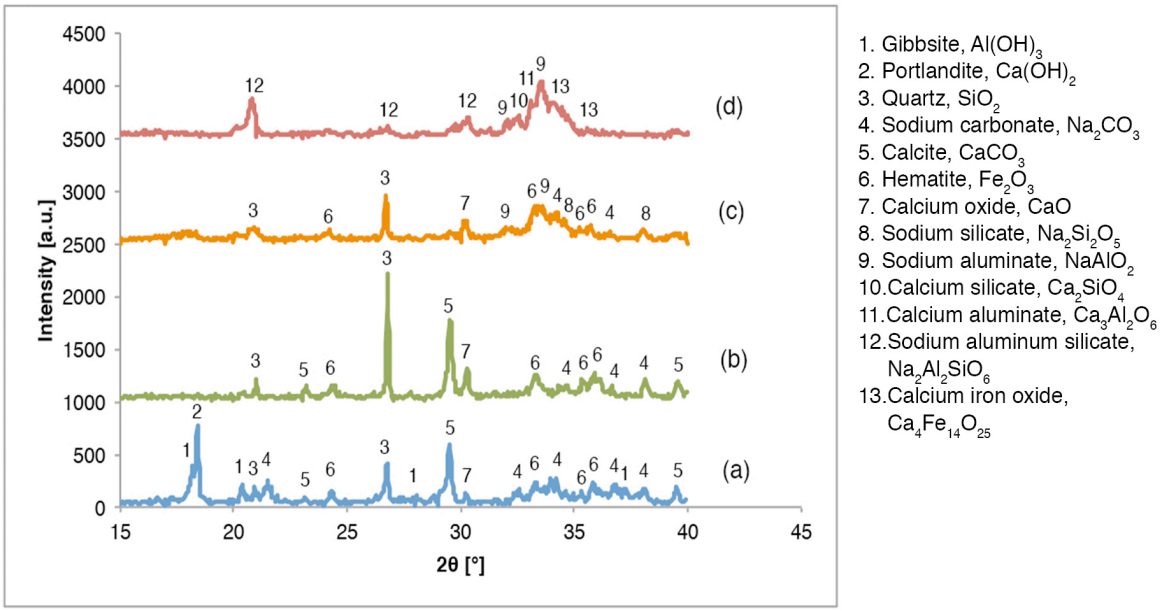

Fig. 2.5. XRD patterns of synthesized catalysts prepared by different calcination temperatures: (a) RSL-uncalcined, (b) RSL-500, (c) RSL-700, (d) RSL-900

According to the XRD pattern shown in **Fig. 2.5d**, calcium aluminate and sodium aluminum silicate were also formed at 900°C. In principle, all of the alumina in the product should be in the form of sodium aluminate. However, the formation of calcium aluminate also occurs in practice [10]. The forming of calcium aluminate might have occurred by the reaction among sodium carbonate, aluminum oxide, and calcium carbonate, while sodium aluminum silicate was formed by further reaction between sodium aluminate with silica. The expression of those reactions can be written as presented in Eqs. (2.7) and (2.8), respectively.

Fig. 2.6 shows the morphologies of the synthesized catalysts. RSL-uncalcined and RSL-500 exhibited distributions of fined particles, as shown in **Fig. 2.6a** and

2.6b, respectively. At higher calcination temperatures, a unique appearance called sponge structures were formed (**Fig. 2.6c** dan **2.6d**). The structures occurred due to agglomeration among red mud, sodium carbonate and limestone during calcination at high temperature. In comparison, calcination of red mud at 900°C with no soda-lime did not change the morphology (**Fig. 2.7**). This means that soda-lime calcination can affect the morphology of catalyst resulting in significant deformation.

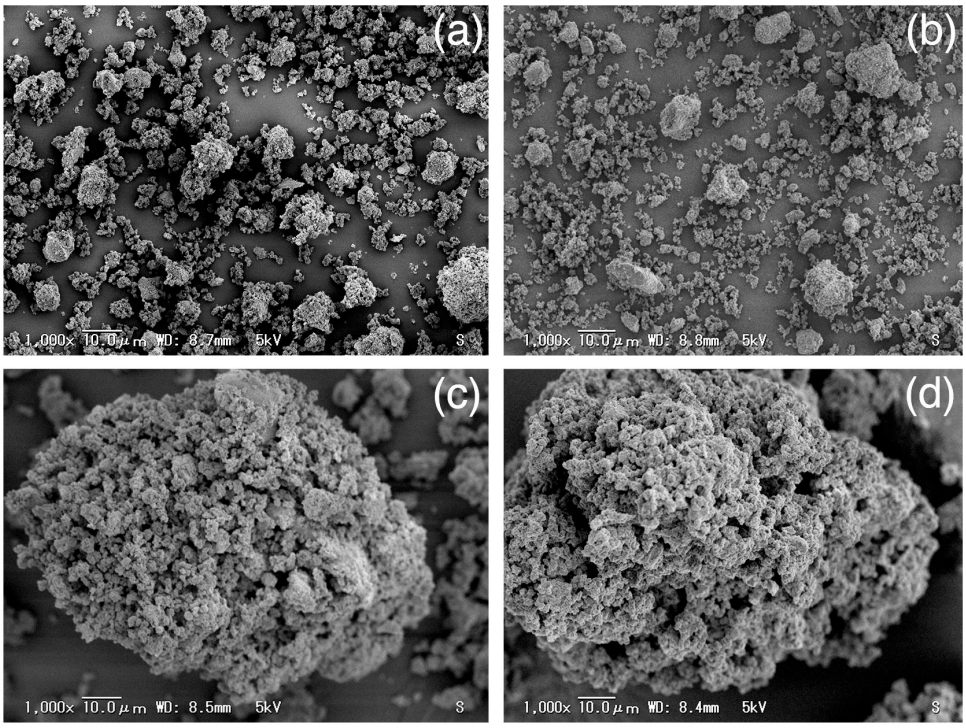

Fig. 2.6. SEM images at 1,000x magnification of synthesized catalyst: (a) RSL-uncalcined, (b) RSL-500, (c) RSL-700, (d) RSL-900

N_2 adsorption analysis measured the specific surface area of the prepared catalysts. This analysis will also prove either the particles were agglomerating or expanding. The specific surface area of the prepared catalysts were 23, 18, 4.3, and 1.3 m^2/g for RSL-uncalcined, RSL-500, RSL-700, and RSL-900, respectively. The result shows that the specific surface area of the prepared catalysts tend to decrease,

and it reveals that the sponge structures were formed due to agglomeration during calcination, instead of expanding.

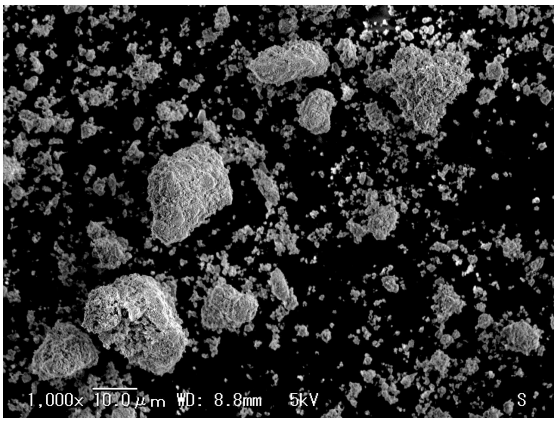

Fig. 2.7. SEM images at 1,000x magnification of red mud calcined at 900°C for 2 h

2.5 Summary

The following are some of the important points discussed in this chapter:

- The presence of sodium carbonate and limestone as additives have significant influence on the crystallinity, morphology, and basicity of the red mud during calcination.
- The crystallite phase transformation occurred during calcination. The intensity of calcium oxide increased at 500°C and 700°C, while sodium aluminate and sodium silicate were formed starting from 700°C.
- As the consequence of the formation of those compounds, the basicity of the prepared catalyst tend to increase with increasing calcination temperature.
- The sponge or porous structures formed due to the agglomeration of the particles during calcination.

References

[1] K. Tanabe, M. Misono, Y. Ono, H. Hattori, New solid acids and bases their catalytic properties, in: B. Delmon, J. Yates (Eds.), Studies in Surface Science and Catalysis, Kodansha Tokyo, Tokyo, 1989: pp. 5–23.

[2] W. Xie, H. Peng, L. Chen, Calcined Mg-Al hydrotalcites as solid base catalysts for methanolysis of soybean oil, Journal of Molecular Catalysis A: Chemical. 246 (2006) 24–32.

[3] K. Tanabe, T. Yamaguchi, Basicity and acidity of solid surfaces, Journal of The Research Institute for Catalysis Hokkaido University. 11 (1964) 179–184.

[4] C. Wu, D. Liu, Mineral phase and physical properties of red mud calcined at different temperatures, Journal of Nanomaterials. 2012 (2012).

[5] N. Datta, S. Chatterji, J.W. Jeffery, A.L. Mackay, On the oriented transformation of $Ca(OH)_2$ to CaO, Mineralogical Magazine. 37 (1969) 250–252.

[6] I. Halikia, L. Zoumpoulakis, E. Christodoulou, D. Prattis, Kinetic study of the thermal decomposition of calcium carbonate by isothermal methods of analysis, The European Journal of Mineral Processing and Environmental Protection. 1 (2001) 89–102.

[7] R. Padilla, H.Y. Sohn, Sintering kinetics and alumina yield in lime-soda sinter process for alumina from coal wastes, Metallurgical Transactions B. 16 (1985) 385–395.

[8] W. Tao, Y. Ping, W. Shenggang, L. Yunbai, Application of sodium aluminate as a heterogeneous base catalyst for biodiesel production from soybean oil, Energy and Fuels. 23 (2009) 1089–1092.

[9] F. Guo, Z.G. Peng, J.Y. Dai, Z.L. Xiu, Calcined sodium silicate as solid base catalyst for biodiesel production, Fuel Processing Technology. 91 (2010) 322–328.

[10] R. Padilla, H.Y. Sohn, Sodium aluminate leaching and desilication in lime-soda sinter process for alumina from coal wastes, Metallurgical Transactions B. 16 (1985) 707–713.

Catalytic Activity of Modified Red Mud Catalyst

The catalytic activity of red mud modified by soda-lime calcination used as a solid base catalyst for transesterification of canola oil was presented in this chapter. The effects of the methanol/oil molar ratio, catalyst amount, reaction temperature, and reaction time were studied to obtain the optimum reaction conditions. Comparison study using different solid base catalyst is also reported in this chapter.

3.1 Transesterification of canola oil

Commercial canola oil was purchased from the market. The catalytic reactions were carried out in a 100mL one-necked round-bottomed flask with a reflux condenser. The flask was immersed in a water-bath equipped with a thermocouple to control the temperature, and a magnetic stirrer was used to stir the solution during the reaction.

The catalytic activity of synthesized catalysts prepared at different calcination temperatures in the transesterification of canola oil with methanol was investigated. The catalyst that showed the highest yield of biodiesel was then used for the subsequent optimization reactions. The parameters considered of the reactions were methanol/oil molar ratio (6:1 to 18:1), catalyst concentration (2 wt% to 6 wt% of the oil), reaction temperature (45–70°C), and reaction time (1–6 h). After the reaction completed, the solid catalyst was separated by simple filtration, then the liquid part was put into a funnel separator and kept for 24 h at room temperature. The liquid

separated into two layers: the upper layer was biodiesel, and the lower layer was glycerol.

3.2 Instrumentation

The yield of biodiesel or fatty acid methyl esters (FAME) of the upper layer was determined by gas chromatography-mass spectrometry (GCMS-QP2010 SE, Shimadzu Corp.) with a Rxi-5Sil MS capillary column (30 m, 0.25 mm, 0.25 μm), using the European procedure EN 14103 [1].

3.3 Catalytic activity of the prepared catalysts

Fig. 3.1 shows the catalytic activity of the catalysts prepared at different calcination temperatures. The catalytic activities of the catalysts initially increased with increasing of calcination temperature, and then decreased, as indicated from the FAME yield. Chapter 2 has discussed the physical and chemical properties of the prepared catalysts. **Table 2.2** shows the catalyst calcined at 900°C had the highest total basicity; however, the highest conversion of canola oil was obtained with the catalyst calcined at 700°C, which gave the highest basicity for H_ in the range of 15.0–17.2. This result was similiar to that obtained with solid-base catalyst described by Guo et al. (2010) [2]. The higher basicity and basic strength represented by H_ (15.0–17.2) could result in the higher activity of the catalyst to produce biodiesel.

During calcination, the crystallite phase transformation from calcium hydroxide to calcium oxide that occurred at the temperature greater than 450°C was due to the dehydration reactions, as presented in Eq. (2.1) [3]. Calcium oxide has better performance as a solid catalyst for transesterification reaction rather than calcium hydroxide and calcium carbonate [4]. Further, sodium silicate and sodium

aluminate started at 700°C (**Fig. 2.5c**, Nos. 8 and 9). Sodium aluminate and sodium silicate have proven to show activity as solid catalyst for the transesterification reaction. Those materials had high basicity and high efficiency for biodiesel production [2,5]. These results support the increase of FAME yield using RSL-700 catalyst.

The increase in temperature and the excess of calcium carbonate made sodium silicate transform into calcium silicate at 900°C (**Fig. 2.5d**, No. 10). Compared to sodium silicate, calcium silicate has lower catalytic activity for biodiesel production. Vorasingha and Sahakitpichan (2015) reported that the highest biodiesel yield using calcium silicate catalyst was only 86% [6].

The morphology of the catalysts also affected to the catalytic activity. During calcination, a unique appearance called sponge structures were formed started at 700°C (**Fig. 2.6c** and **2.6d**). The structures occurred due to agglomeration among red mud, sodium carbonate and limestone during calcination. Agglomeration structures with spaces between agglomerates were reported to be effective solid catalysts for transesterification reaction [7]. The channels containing basic sites at the internal surface can be optimized as the entry of triglyceride and methanol [2]. However, agglomeration causes the surface area to decrease. Moreover, heat treatment with soda-lime could form sintered product at temperatures higher than 900°C [8]. It indicates that some channels are already plugged and the activity of the catalyst would decrease.

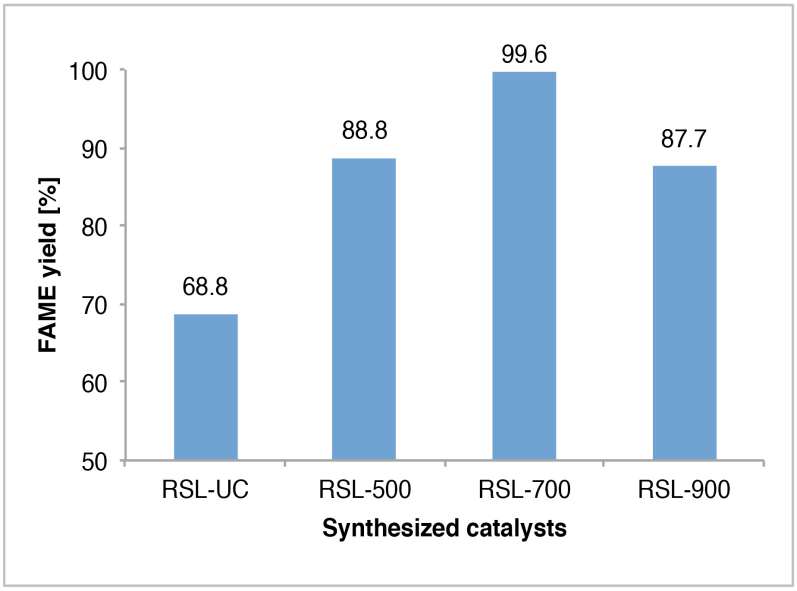

Fig. 3.1. Catalytic activity of the catalysts prepared at different calcination temperatures

Fig. 3.1 also shows that catalyst affected the reaction rate. All the reactions were conducted in the same reaction time (2 h) but the yield obtained were different. It means the reaction rate using RSL-700 is faster than using other prepared catalysts. However, if the reaction is conducted in longer time, it is possible for other prepared catalysts to reach the same optimum point of FAME yield (99.6%).

Kawashima et al. [9] carried out transesterification of rapeseed oil using three different catalyst: KOH (homogeneous catalyst), activated CaO (heterogeneous catalyst), and non-activated CaO (heterogeneous catalyst) (**Fig. 3.2**). The basicity of those catalysts were: KOH > activated CaO > non-activated CaO. They reported that each catalyst has different activity to catalysis the reaction. The higher basicity, the faster reaction rate conducted. However, the catalyst which has weak basicity (non-activated CaO) could reach the optimum point of FAME yield close to that of using KOH, when the reaction was conducted in a longer time. So it reveals that catalyst affected the reaction rate.

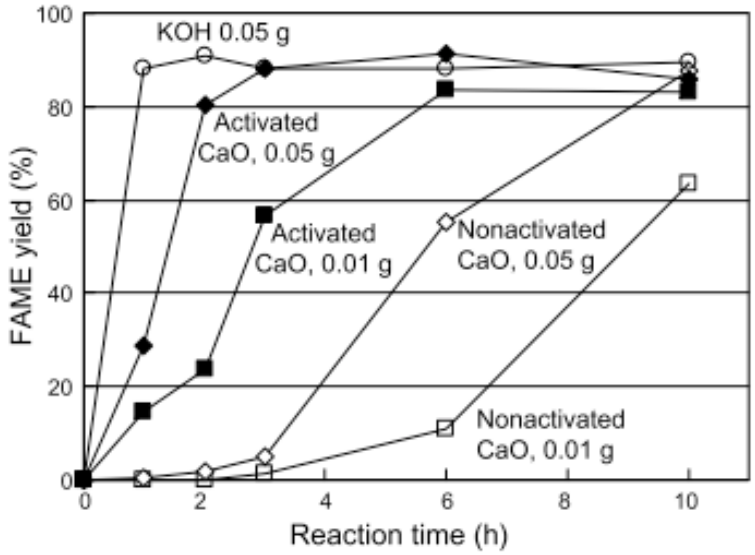

Fig. 3.2. Catalytic activity of KOH, activated CaO, and non-activated CaO in transesterification of rapeseed oil with methanol at 60°C [9]

3.4 Effects of transesterification reaction variables

The FAME yield was affected by transesterification reaction variables such as the molar ratio of methanol/oil, catalyst amount, reaction temperature and reaction time. In this section, the effect of reaction variables was investigated in the presence of the catalyst to obtain the optimum reaction conditions. RSL-700 was used for the following reactions because it had the highest performance compared to the other prepared catalysts.

3.4.1 Effect of methanol/oil molar ratio

Fig. 3.3 shows the effect of methanol/oil molar ratio. The FAME yield increased with the increase of the methanol/oil molar ratio, and reached a maximum value when the ratio was 12:1. Stoichiometrically, 3 mol of methanol is required for each mole of triglyceride, but the excess of methanol is important to shift the

equilibrium of the reaction to produce more methyl esters [4-7]. However, further excess of methanol more than the optimum point was not preferable to the reaction.

In principle, glycerol is not soluble in FAME, while methanol is completely soluble in both FAME and glycerol. By the excess of methanol in the system, the solubility of glycerol and FAME in methanol will increase, and lead a portion of diluted glycerol remaining in the FAME phase. Such conditions lead the difficulties of FAME-glycerol separation [10,11].

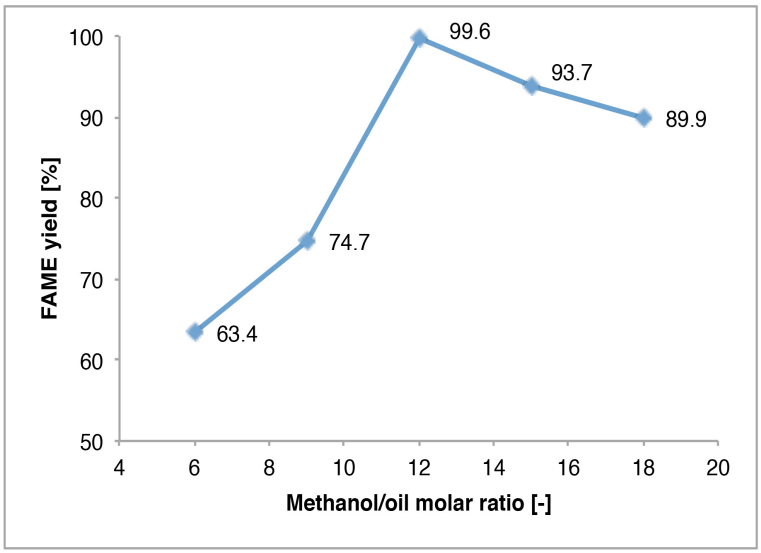

Fig. 3.3. Effect of methanol/oil molar ratio on the FAME yield (reaction conditions: catalyst amount of 4 wt%, temperature of 60°C, and reaction time of 2 h)

3.4.2 Effect of catalyst amount

The effect of catalyst amount was studied by varying the amount of the catalyst in the range of 2–6 wt%. The FAME yield increased with the increase of catalyst amount, and reached a maximum value at 4 wt% concentration (**Fig. 3.4**).

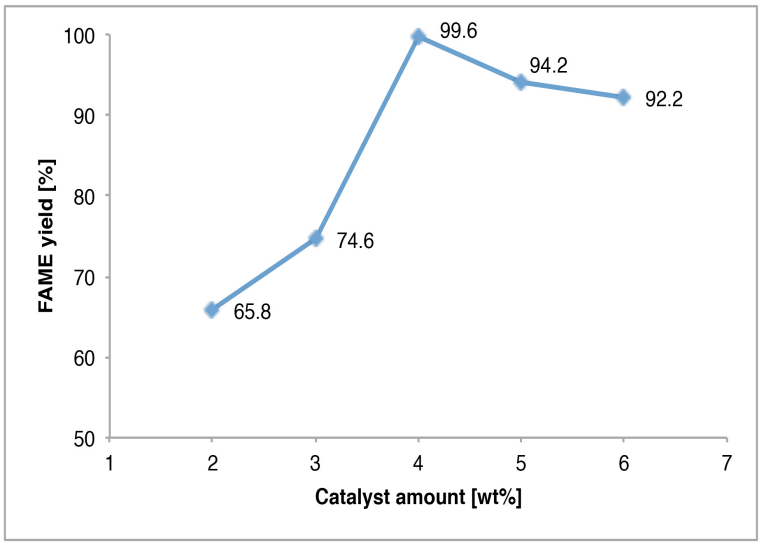

Fig. 3.4. Effect of catalyst amount on the FAME yield (reaction conditions: methanol/oil molar ratio of 12:1, temperature of 60°C, and reaction time of 2 h)

Base catalysts play an important role to deprotonate methanol into methoxide ion ($^{-}OCH_3$), a nucleophilic species. This species can easily attack triglyceride molecules to produce methyl esters (biodiesel) [12]. Therefore, with higher catalyst concentration in the mixture, a higher amount of methyl ester is produced. However, the excess catalysts would cause soap formation because of the reaction of high concentration alkali metals from the catalyst with esters and triglycerides [13,14]. Then the soap formation would increases the viscosity of the solutions, which makes mixing difficult, resulted the decrease of biodiesel yield.

3.4.3 Effect of reaction temperature

Fig. 3.5 shows the effect of reaction temperature to the FAME yield. Initially, the yield increased and reached the optimal point at 60ºC. Generally, the methanolysis reaction occurrs close to the boiling point of methanol [9]. Methanol starts to boil at 65ºC at atmospheric pressure, so at that temperature and higher, the conversion of oil would not occur well. Ragit et al. and Abbah et al. [15,16] reported that such

condition is due to some methanol evaporation which caused the decrease of the FAME yield. Besides that, the other possible reason is the oxidation of the catalyst surface at higher temperature. This condition will destruct the catalyst surface and decrease its activity.

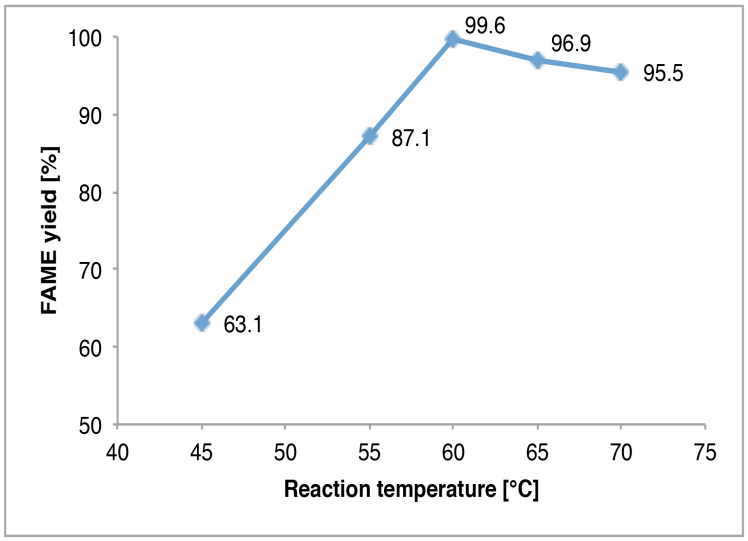

Fig. 3.5. Effect of reaction temperature on the FAME yield (reaction conditions: methanol/oil molar ratio of 12:1, catalyst amount of 4 wt%, and reaction time of 2 h)

3.4.4 Effect of reaction time

To study the effect of reaction time, a series of experiments was conducted in the range of 1–6 h. **Fig. 3.6** shows that the FAME yield increased in the initial stages of reaction. After reaching the optimal point at 2 h, the yield of biodiesel then decreased. Transesterification is a reversible reaction and involves three-step reaction. It needs sufficient reaction time to complete the reactions until it reaches the optimum point. However, a longer reaction time will cause more soap formation due to reaction of alkali from the catalyst with esters and triglycerides. Further, soap formation will cause difficulties in biodiesel separation [17].

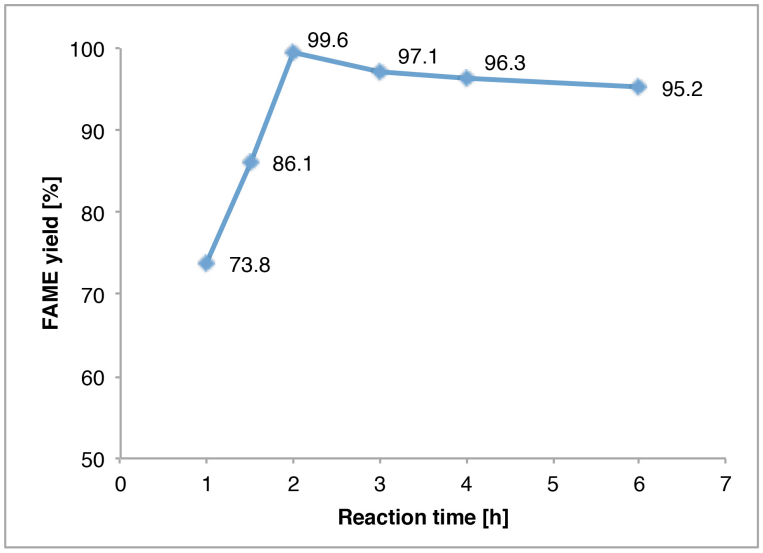

Fig. 3.6. Effect of reaction time on the FAME yield (reaction conditions: methanol/oil molar ratio of 12:1, catalyst amount of 4 wt%, and temperature of 60°C)

3.5 Comparison of FAME yield using different solid base catalyst

As a comparison study, calcium oxide of laboratory grade (Wako Pure Chemical Industries, Ltd.) was used as a solid catalyst using the optimum reaction condition. Calcium oxide is the most common solid base catalyst used in research of biodiesel production [4]. Prior to being used, the calcium oxide was calcined at 700°C for 2 h to remove any contamination of carbonates and hydroxides. The catalytic activity of calcium oxide was lower than the activity of RSL-700 for transesterification of canola oil, with a FAME yield of 94.3% and 99.6%, respectively (**Fig. 3.7**).

RSL-700 had a higher catalytic activity than calcium oxide due to RSL-700 containing sodium aluminate and sodium silicate as active compounds. According to the previous studies, the activity of sodium aluminate and sodium silicate for transesterification reaction were higher than calcium oxide [2,4,7]. Furthermore, the basicity test using Hammett indicators reveals that RSL-700 had a higher basic

strength than calcium oxide, with H_ in the range of 15.0–17.2 and 9.8–15.0, respectively.

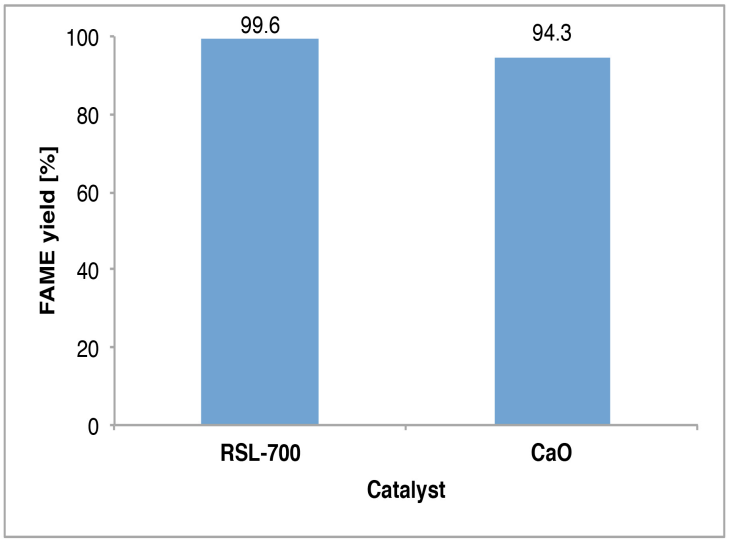

Fig. 3.7. Catalytic activity of RSL-700 and CaO using optimum reaction conditions

By using red mud as a raw material for biodiesel catalyst, there would be obtaining some benefits: (1) the process could be made economical due to the use of low-cost waste material, (2) environmentally friendly process could be promoted by recycling the waste.

3.6 Possibility of using the catalyst for other plant oils

Generally, one catalyst can be used for some different plant oils in transesterification reaction. Anastopoulos et al. [18] reported that transesterification of sunflower oil, rapeseed oil, olive oil, and used frying oil using NaOH catalyst could produce biodiesel, but with different ester content (**Table 3.1**). The variation of the esters content obtained was due to the difference of fatty acid composition of each plant oils.

Table 3.1. Ester content produced from transesterification of sunflower oil, rapeseed oil, olive oil, and used frying oil using NaOH catalyst [18]

Oil ethyl esters	Sunflower oil ethyl esters	Rapeseed oil ethyl esters	Olive oil ethyl esters	Used frying oil ethyl esters
Ester content (%)	96.7	97.2	97.8	93.2

Table 3.2 shows the fatty acid composition of sunflower oil, rapeseed oil, olive oil, and used frying oil [18]. There are two types of fatty acids: saturated fatty acid and unsaturated fatty acid. Saturated fatty acid, such as lauric acid, palmitic acid, stearic acid, behenic acid, and ligoneceric acid, have higher viscosities compared to unsaturated fatty acids. Such conditions make the oil which contains high saturated fatty acid (used frying oil; saturated fatty acid > 20%) more difficult to be reacted compared to others that contain low saturated fatty acid (sunflower, rapeseed, and olive oil; saturated fatty acid < 15%).

Table 3.2. Fatty acid composition of sunflower oil, rapeseed oil, olive oil, and used frying oil (wt%) [18]

Fatty acid	Chemical structure	Sunflower oil	Rapeseed oil	Olive oil	Used frying oil
Lauric	$CH_3(CH_2)_{10}COOH$	0.00	0.00	0.00	1.98
Palmitic	$CH_3(CH_2)_{14}COOH$	6.20	4.90	11.60	15.65
Palmitoleic	$CH_3(CH_2)_5CH=CH(CH_2)_7COOH$	0.10	0.00	0.90	0.31
Stearic	$CH_3(CH_2)_{16}COOH$	3.70	1.60	3.10	3.10
Oleic	$CH_3(CH_2)_7CH=CH(CH_2)_7COOH$	25.20	33.00	74.98	29.57
Linoleic	$CH_3(CH_2)_3(CH_2CH=CH)_2(CH_2)_7COOH$	63.10	20.40	7.80	41.53
Linolenic	$CH_3(CH_2CH=CH)_3(CH_2)_7COOH$	0.30	7.90	0.60	1.04
Eicosenoic	$CH_3(CH_2)_8CH=CH(CH_2)_8COOH$	0.20	9.30	0.01	0.11
Behenic	$CH_3(CH_2)_{20}COOH$	0.70	0.00	0.10	0.24
Erucic	$CH_3(CH_2)_7CH=CH(CH_2)_{11}COOH$	0.10	23.0	0.00	0.02
Lignoceric	$CH_3(CH_2)_{22}COOH$	0.20	0.00	0.50	0.30

According to those results, it is possible to use the prepared catalyst (modified red mud catalyst) for some plant oils to produce biodiesel. The most important properties to be considered is the composition of fatty acid of the plant oils. The less content of saturated fatty acid, the easier reaction could be conducted.

3.7 Summary

The following are some of the important points discussed in this chapter:

- RSL-700 exhibited the highest catalytic activity among the as-synthesized catalysts because it has high basic strength, contains sodium silicate and sodium aluminate, and have sponge structures that is suitable for transesterification reaction.
- The optimum reaction conditions of transesterification of canola oil were the following: 12:1 methanol/oil molar ratio, 4 wt% catalyst amount, 60°C reaction temperature, and 2 h reaction time, which resulted to 99.6% FAME yield.
- The catalytic activity of RSL-700 was higher than the activity of calcium oxide for transesterification of canola oil.

References

[1] European Committee for Standardization, EN-14103: Determination of ester and linolenic acid methyl ester contents, Brussels, Belgium, 2003.

[2] F. Guo, Z.G. Peng, J.Y. Dai, Z.L. Xiu, Calcined sodium silicate as solid base catalyst for biodiesel production, Fuel Processing Technology. 91 (2010) 322–328.

[3] N. Datta, S. Chatterji, J.W. Jeffery, A.L. Mackay, On the oriented transformation of $Ca(OH)_2$ to CaO, Mineralogical Magazine. 37 (1969) 250–252.

[4] M. Kouzu, T. Kasuno, M. Tajika, Y. Sugimoto, S. Yamanaka, J. Hidaka, Calcium oxide as a solid base catalyst for transesterification of soybean oil and its application to biodiesel production, Fuel. 87 (2008) 2798–2806.

[5] W. Tao, Y. Ping, W. Shenggang, L. Yunbai, Application of sodium aluminate as a heterogeneous base catalyst for biodiesel production from soybean oil, Energy and Fuels. 23 (2009) 1089–1092.

[6] A. Vorasingha, P. Sahakitpichan, Biodiesel Production by using Calcium Silicate ($CaSiO_3$) as Heterogeneous Catalyst, in: Burapha University International Conference 2015, 2015: pp. 789–797.

[7] S.K. Cherikkallinmel, A. Gopalakrishnan, Z. Yaakob, R.M. Ramakrishnan, S. Sugunan, B.N. Narayanan, Sodium aluminate from waste aluminium source as catalyst for the transesterification of Jatropha oil, RSC Adv. 5 (2015) 46290–46294.

[8] R. Padilla, H.Y. Sohn, Sintering Kinetics and Alumina Yield in Lime-Soda Sinter Process for Alumina from Coal Wastes, Metallurgical Transactions B. 16 (1985) 385–395.

[9] A. Kawashima, K. Matsubara, K. Honda, Acceleration of catalytic activity of calcium oxide for biodiesel production, Bioresource Technology. 100 (2009) 696-700.

[10] H. Zhou, H. Lu, B. Liang, Solubility of multicomponent system in the biodiesel production by transesterification of *Jatropha curcas* L. oil with methanol, Journal of Chemical and Engineering Data. 51 (2006) 1130-1135.

[11] I. A. Musa, The effects of alcohol to oil molar ratios and the type of alcohol on biodiesel production using transesterification process (review), Egyptian Journal of Petroleum. 25 (2016) 21-31.

[12] H. V Lee, J.C. Juan, N.F. Binti Abdullah, R. Nizah Mf, Y.H. Taufiq-Yap, Heterogeneous base catalysts for edible palm and non- edible Jatropha- based biodiesel production, Chemistry Central Journal. 8 (2014) 1–9.

[13] A. Singh, B. He, J. Thompson, J. Van Gerpen, Process optimization of biodiesel production using alkaline catalysts, Applied Engineering in Agriculture. 22 (2006) 597–600.

[14] F. Yang, Y. Su, X. Li, Q. Zhang, R. Sun, Preparation of biodiesel from *Idesia polycarpa* var. *vestita* fruit oil, Industrials Crops and Products. 29 (2009) 622-628.

[15] S.S. Ragit, S.K. Mohapatra, K. Kundu, P. Gill, Optimization of neem methyl ester from transesterification process and fuel characterization as a diesel substitute, Biomass and Bioenergy. 35 (2010) 1138–1144.

[16] E.C. Abbah, G.I. Nwandikom, C.C. Egwuonwu, N.R. Nwakuba, Effect of Reaction Temperature on the Yield of Biodiesel From Neem Seed Oil, American Journal of Energy Science. 3 (2016) 16–20.

[17] A.F. Lee, J. a Bennett, J.C. Manayil, K. Wilson, Heterogeneous catalysis for sustainable biodiesel production via esterification and transesterification, Chemical Society Reviews. 43 (2014) 7887–7916.

[18] G. Anastopoulos, Y. Zannikou, S. Stournas, S. Kalligeros, Transesterification of vegetable oils with ethanol and characterization of the key fuel properties of ethyl esters, Energies. 2 (2009) 362-376.

Chapter 4

Study on Deactivation and Regeneration of Catalyst

The deactivation of modified red mud catalyst was studied to determine which factors are responsible to degradation of its properties and activities. The regeneration of the deactivated catalyst was conducted by calcination, washing with hexane, and combination of them to determine the most effective method to recover its catalytic activity. The activity of the deactivated and regenerated catalyst were tested in the transesterification of canola oil. The physical and chemical properties of the catalysts such as thermogravimetry behaviour, crystallinity, morphology, specific surface area, and basic strength are also presented in this chapter.

4.1 Catalyts regeneration

RSL-700 was used as the fresh catalyst and labelled as FC. The deactivated or used catalyst was dried at 100°C overnight and labelled as DUC. The used catalysts were then regenerated through three different methods. First, the DUC was calcined at 700°C for 2 h, labelled as DUC-cal. Second, the used catalyst was washed using hexane and dried at 100°C overnight, labelled as WUC. Third, the WUC was calcined at 700°C for 2 h, labelled as WUC-cal. The deactivated and regenerated catalysts were then tested for their catalytic activity through transesterification of canola oil according to the procedure mentioned in Chapter 4.

4.2 Instrumentation

Characterization of the recovered catalyst was conducted using various methods. Crystallinity and mineral contents identification was conducted using X-ray diffraction (XRD) Rigaku Multiflex X-ray diffractometer with Cu-Kα radiation (λ = 1.54056Å) at 40 kV, 20 mA over the 2-theta range of 15–40˚. Thermogravimetry analysis were determined using Rigaku Thermoplus TG 8120 under air flow at a heating rate of 10˚C/min up to 900˚C. The basic strength of the catalyst was estimated using bromothymol blue (H_=7.2), phenolphthalein (H_=9.3), 2,4-dinitroaniline (H_=15.0), and 4-chloro-2-nitroaniline (H_=17.2) as Hammett indicators [1,2]. Scanning electron microscope (SEM) image was obtained using Keyence VE-8800 for morphological observation. Specific surface area of the catalyst was measured using N_2 adsorption Autosorb-1C (Quantachrome Instruments, AX1C-MP-LP) and calculated using the BET method. Inductively coupled plasma atomic emission spectroscopy (ICP-AES, Seiko Instruments Inc., SPS 7800) was used to determine the percentage of Na in the catalyst. The FTIR spectrum was recorded using Jasco FT/IR-6100FV in the region of 500–4000 cm^{-1}.

4.3 Catalytic activity of the catalysts

Fig. 4.1 shows the catalytic activity of the fresh, deactivated, and regenerated catalysts used in transesterification of canola oil. The catalytic activity of deactivated catalyst decreased significantly compared to the fresh one. The FAME yield of the produced biodiesel were 48.9% and 99.6%, respectively. After regeneration by calcination, the FAME yield of the produced biodiesel increased up to 78.9%. By washing with hexane and in combination with calcination, the activity were even higher. The FAME yield were 81.8% and 96.8%, respectively. It showed that washing

with hexane is an effective method to recover the catalyst activity. Further, by combining with calcination, the performance of the catalyst return almost as high as the fresh catalyst. The physical and chemical properties of the catalysts will be discussed more detail in section 5.6 to answer the question which factors are responsible in the degradation of the catalyst properties and activities.

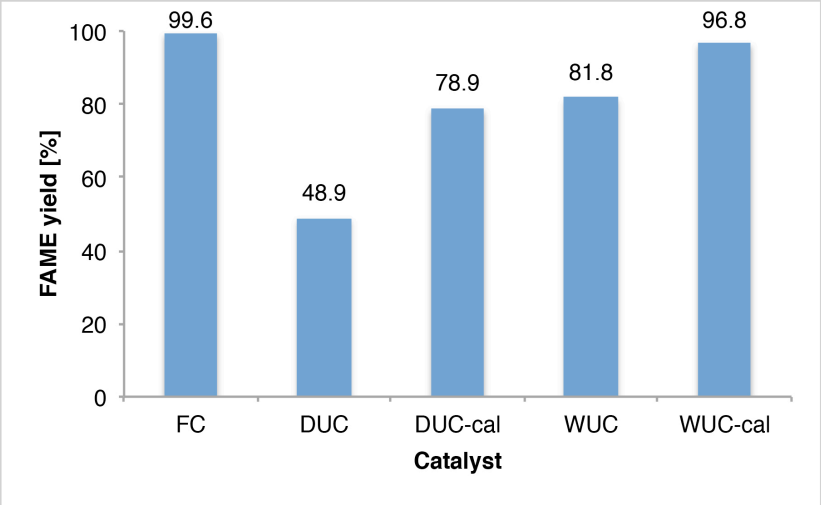

Fig. 4.1. FAME yield of transesterification of canola oil over the catalysts (reaction conditions: methanol/oil molar ratio of 12:1, catalyst amount of 4%, temperature of 60˚C, and reaction time of 2 h)

4.4 Effect on physical and chemical properties

In this section, the physical and chemical properties of the deactivated and regenerated catalysts such as thermogravimetry behaviour, chemical bond structure, crystallinity, morphology, specific surface area, and basic strength were investigated.

4.4.1 Thermogravimetry behavior

Fig. 4.2 shows the TG profiles of the catalysts. Each catalyst had different weight loss in the range from room temperature to 900˚C. The fresh catalyst had

nearly no weight loss up to 700˚C and slight loss at 900˚C. The significant weight loss of about 40% occured in the deactivated catalyst, due to deposition of organic compounds from the working solution. It revealed that the organic deposits the main cause of catalyst deactivation [3,4]. This result support the fact of its decrease in catalytic activity. The regerenerated catalyst by calcination or by washing with hexane shows weight loss about 20% due to the remaining deposition of organic compounds from the solution. The contaminants can be released effectively by washing and followed by calcination, and it was indicated by the TG profile which showed very slight weight loss during heating.

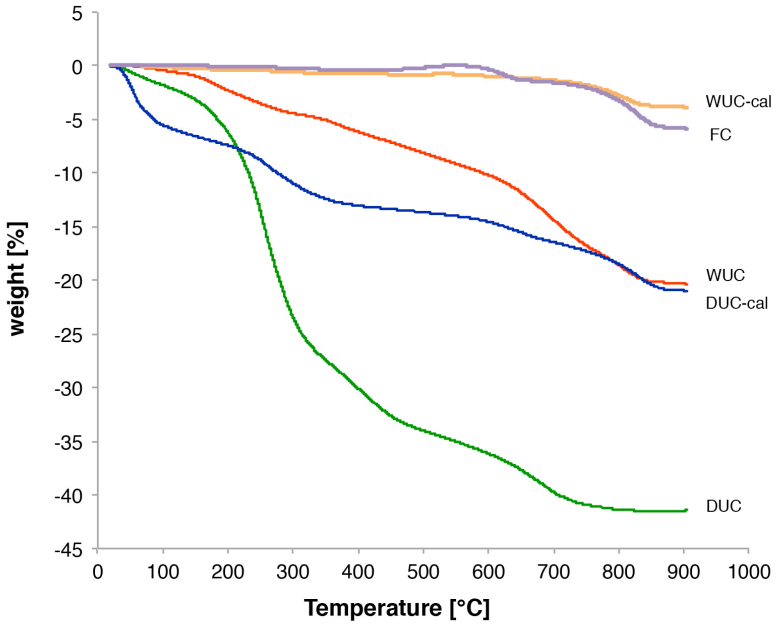

Fig. 4.2. TG profiles of the fresh, deactivated, and regenerated catalysts

4.4.2 Chemical bond structure

To study the reason for the decrease of FAME yield, FTIR spectroscopy was used to explain the change of chemical bond structure on the catalyst surface. The change can be caused by surface interaction with constituents such as residues or

products of the reactions. **Fig. 4.3** shows the FTIR spectra of the catalysts. In the case of fresh catalyst (**Fig. 4.3a**), a sharp band was observed at 3644 cm^{-1}, due to the vibration of the OH groups that attached to Ca^{2+} and Na^{+}. This could be assigned to the OH group vibrations of the bound H_2O on the surface of the sample. In addition, the band at 1674 cm^{-1} confirmed the adsorption of water on the catalyst surface [5]. The bands around 1445, 989, and 881 cm^{-1} represent the vibrations of the carbonates ion [6]. The carbonate species derived from the interaction between the surface basic sites with CO_2 from the atmosphere [5]. The FTIR spectra of regenerated catalysts (**Fig. 4.3c-e**) still retained the characteristic spectra of the fresh one, and almost no significant changes during regeneration processes.

The significant change of the FTIR spectra occured in the deactivated catalyst (**Fig. 4.3b**). The deactivated catalyst presented new bands in the range of 2950–2850 cm^{-1}, corresponds to the C-H vibrations [5]. New bands were also observed at around 1745 and 1561 cm^{-1}, which were associated with the C=O group vibrations [7]. All the new bands resulted from the adsorption of methyl esters, glycerides, or glycerol on the catalyst surface, as the products and by-products of transesterication reaction [8]. These results revealed that after reaction, the contaminants still attached on the catalyst surface and affected the availability of its active compounds. Such conditions made the catalyst loss its activity.

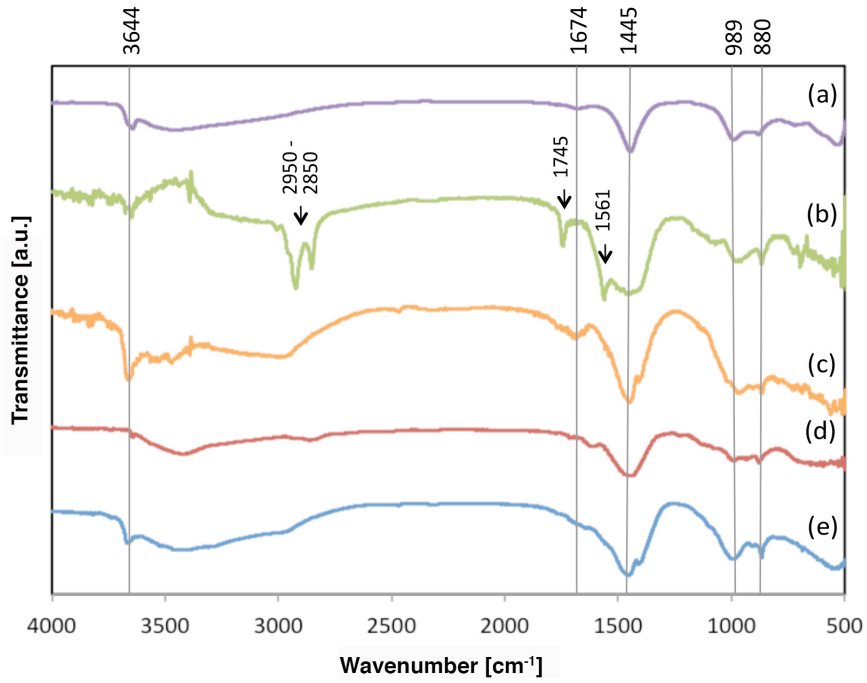

Fig. 4.3. FTIR spectra of the catalysts: (a) FC, (b) DUC, (c) DUC-cal, (d) WUC, (e) WUC-cal

4.4.3 Morphology and specific surface area

Fig. 4.4 shows the morphology of the catalysts. The fresh catalyst exhibited spongy and porous structures indicating surfaces with high adsorption capability. The particles shown have uniform distribution of agglomerates with irregular shapes (**Fig. 4.4a**). Agglomeration structures with spaces between agglomerates are effective solid catalysts for transesterification [9]. The channels can be optimized for the entry of triglyceride and methanol during reaction which contains basic sites at the internal surface [10]. After the reaction, the deactivated catalyst appeared to be more dense (**Fig. 4.4b**). The physical changes occured due to covarage of the active sites by contaminants, which had significant effect on the loss of catalytic activity [11]. The regeneration by calcination improved the catalyst surfaces by burning out the deposited organic compounds as shown in **Fig. 4.4c**. On the other hand by washing

with hexane, and in combination with calcination, produced porous structures with high distribution of agglomerates (**Fig. 4.4d** and **e**). The treatments made the active sites exposed and easily accessed by the reactants during reaction, indicated by the increase of FAME yield (**Fig. 4.1**).

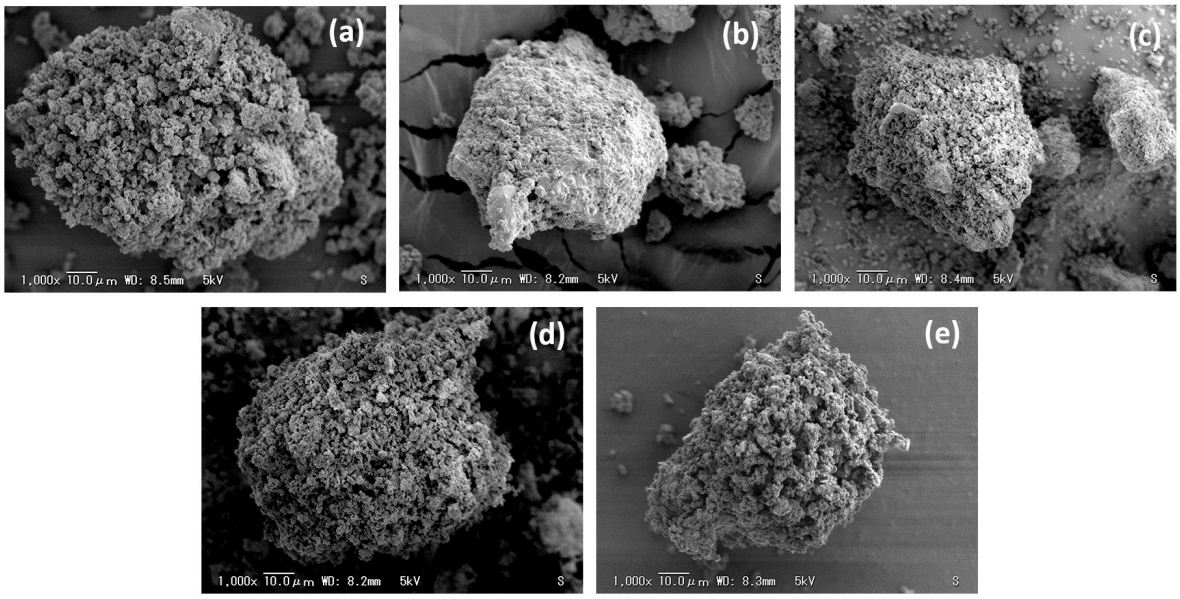

Fig. 4.4 SEM images at 1,000 magnification of the catalysts: (a) FC, (b) DUC, (c) DUC-cal, (d) WUC, (e) WUC-cal

The N_2 adsorption analysis supported the SEM results as shown in **Table 4.1**. The specific surface area of deactivated catalyst decreased significantly from 4.45 m^2/g (fresh catalyst) to 0.94 m^2/g. Researchers had investigated the reason behind the loss in catalytic activity from the fresh to deactivated catalyst. They concluded that the loss of catalytic activity could be related to the decrease of the specific surface area of the deactivated catalyst [12,13]. The regeneration of deactivated catalyst by washing and/or calcination effectively increased the specific surface area due to liberation of the surface from the contaminants, which considerably increased the catalytic activity.

Table 4.1. Specific surface area and basic strength of the catalysts

Catalyst	Specific surface area, BET [m^2/g]	Basic strength [H_]
FC	4.45	15.0−17.2
DUC	0.94	7.2−9.3
DUC-cal	2.71	9.3−15.0
WUC	6.36	9.3−15.0
WUC-cal	10.18	15.0−17.2

4.4.4 Crystallinity and basic strength

Fig. 4.5 shows the XRD patterns of the catalysts. The XRD pattern of the fresh catalyst shows some active compounds for transesterification reaction, such as calcium oxide, sodium aluminate, and sodium silicate (**Fig. 4.5a**). Those compounds were reported to have high basicity and high activity as solid catalyst for biodiesel production [10,14,15]. Basicity or basic strength in biodiesel catalyst has important role to deprotonate methanol into methoxide ion ($^{-}OCH_3$), a species that can reacts with triglyceride to form methyl esters (biodiesel) [16]. The higher basic strength of the catalyst the higher its catalytic activity.

The XRD pattern of deactivated catalyst shows significant decrease in the active compounds' relative intensity to quartz peak (**Fig. 4.5b**). Some of them also disappeared due to obstruction of the catalyst surface by contaminants. This phenomenon was also reported by Dias et al. and Deng et al. [17,18]. Such conditions led to the low accessibility of the active sites to the reactants, as indicated by the decrease of its basic strength using Hammet indicators (**Table 4.1**). The regeneration by calcination improved the crystallinity of the catalyst. Some active compounds appeared but the intensity was still low (**Fig. 4.5c**). The catalyst structures improved

by washing with hexane, followed by calcination as shown in **Fig. 4.5d** and **e**, respectively. The intensity of the active compounds increased as well as the basic strength as shown in **Table 4.1**, and affected its catalytic activity.

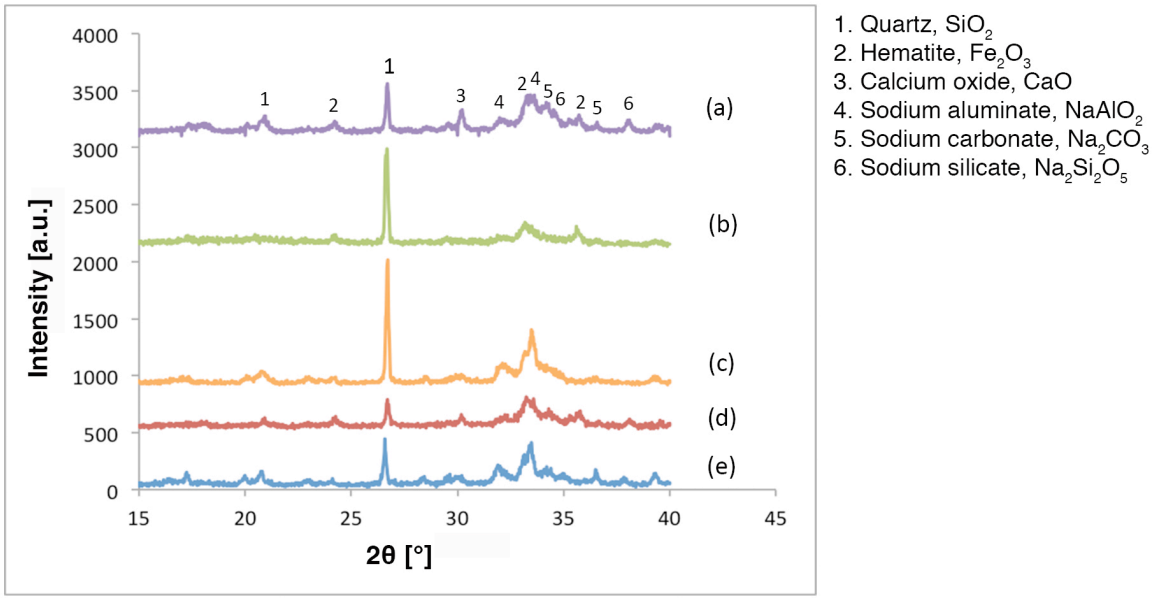

Fig. 4.5. XRD patterns of the catalysts: (a) FC, (b) DUC, (c) DUC-cal, (d) WUC, (e) WUC-cal

4.4.5 Na content

From ICP-AES, it was observed that the content of Na in the fresh and deactivated catalyst were 23.55% and 17.36% respectively. But after calcining the deactivated catalyst at 700 °C, the content of Na in the catalyst was found to be 22.76%. It means a most of the residue were burned and released from the catalyst, and there was no significant loss of Na occurred.

4.5 Reusability of catalyst

The reusability of the catalyst was tested by repeating the transeseterification reaction using the used catalyst. The catalyst was separated by filtration, washed with hexane, and calcined at 700°C for 2 h. **Fig. 4.6** shows that the used catalyst still had high activity after 3 times of reuse. As explained before, one of the important factors for biodiesel production is the basicity of the catalyst. According to the basicity test using Hammett indicators, the regenerated catalyst still showed high basic strength with H_ in the range of 15.0–17.2.

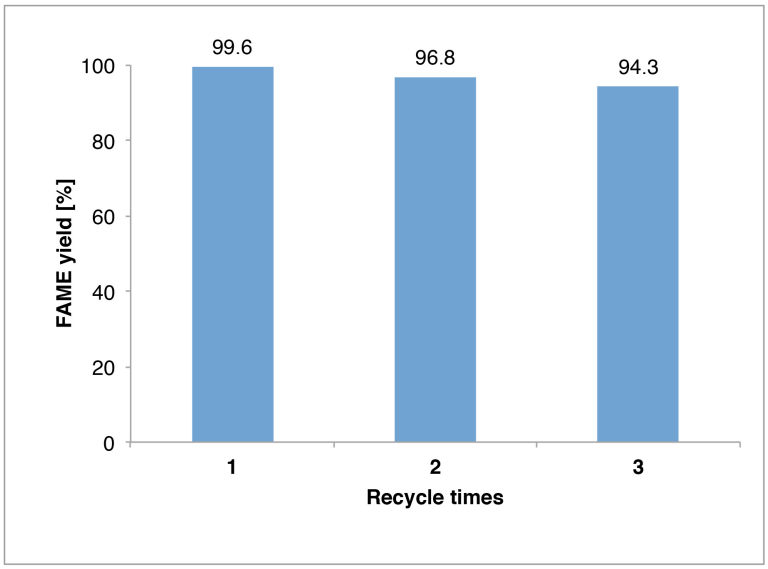

Fig. 4.6. Effect of reusability of catalyst on the FAME yield (reaction conditions: methanol/oil molar ratio of 12:1, catalyst amount of 4%, temperature of 60˚C, and reaction time of 2 h)

4.6 Comparison study: Regeneration of modified red mud catalyst and CaO based catalysts

Calcium oxide is the most common solid base catalyst used in research of biodiesel production [4]. **Table 4.2** summarizes the performance of regenerated CaO

based catalysts in biodiesel production using different regeneration methods. The performance of regenerated modified red mud catalyst prepared in this study was also presented. Compared to the regenerated CaO based catalyst, regenerated modified red mud catalyst had better performance. The FAME yield for repeated use shows high value without any significant loss of activity.

Table 4.2. Regeneration of CaO based catalyst and modified red mud catalyst, and their performance used in transesterification reaction

Catalyst	Regeneration process (washing with solvent, calcination temperature)	FAME yield [%]	Ref.
CaO from mud clam shells	n-hexane, 900°C	96.7 to 74.5	[19]
CaZnO	n-hexane, MeOH, 800°C (3 h)	80 to <80	[20]
CaO from biomass	Acetone, EtOH, 600°C–800°C (4 h)	75 to 50	[21]
CaO from waste cockle shells	MeOH, n-hexane , 900°C (2 h)	>97	[22]
Modified red mud	n-hexane, 700°C (2 h)	99.6 to 96.8	This study

4.7 Summary

The following are some of the important points discussed in this chapter:

- Deactivation of modified red mud catalyst used in transesterification reaction was mainly due to deposits of organic compounds on the catalyst.
- The results from TG, FTIR, XRD, and SEM showed that the contaminants changed the properties of the catalyst.

- The deposited organic compounds in the catalyst decreased the specific surface area as well as the basic strength of the catalyst, and considerably reduced its catalytic activity.
- Regeneration by washing the used catalyst with hexane and calcination can recover its catalytic activity close to that of the fresh one.

References

[1] K. Tanabe, M. Misono, Y. Ono, H. Hattori, New solid acids and bases their catalytic properties, in: B. Delmon, J. Yates (Eds.), Studies in Surface Science and Catalysis, Kodansha Tokyo, Tokyo, 1989: pp. 5–23.

[2] W. Xie, H. Peng, L. Chen, Calcined Mg-Al hydrotalcites as solid base catalysts for methanolysis of soybean oil, Journal of Molecular Catalysis A: Chemical. 246 (2006) 24–32.

[3] Z. Wen, X. Yu, S.-T. Tu, J. Yan, E. Dahlquist, Biodiesel production from waste cooking oil catalyzed by TiO2-MgO mixed oxides, Bioresource Technology. 101 (2010) 9570–9576.

[4] M. Kouzu, J.S. Hidaka, Transesterification of vegetable oil into biodiesel catalyzed by CaO: A review, Fuel. 93 (2012) 1–12.

[5] F.J. Li, H.Q. Li, L.G. Wang, Y. Cao, Waste carbide slag as a solid base catalyst for effective synthesis of biodiesel via transesterification of soybean oil with methanol, Fuel Processing Technology. 131 (2015) 421–429.

[6] J.D. Rodriguez-Blanco, S. Shaw, L.G. Benning, The kinetics and mechanisms of amorphous calcium carbonate (ACC) crystallization to calcite, via vaterite, Nanoscale. 3 (2011) 265–271.

[7] J. Coates, Interpretation of Infrared Spectra , A Practical Approach, in: R.A. Meyers (Ed.), Encyclopedia of Analytical Chemistry, John Wiley & Sons Ltd, Chichester, 2000: pp. 10815–10837.

[8] M. Verziu, S.M. Coman, R. Richards, V.I. Parvulescu, Transesterification of vegetable oils over CaO catalysts, Catalysis Today. 167 (2011) 64–70.

[9] S.K. Cherikkallinmel, A. Gopalakrishnan, Z. Yaakob, R.M. Ramakrishnan, S. Sugunan, B.N. Narayanan, Sodium aluminate from waste aluminium source as catalyst for the transesterification of Jatropha oil, RSC Adv. 5 (2015) 46290–46294.

[10] F. Guo, Z.G. Peng, J.Y. Dai, Z.L. Xiu, Calcined sodium silicate as solid base catalyst for biodiesel production, Fuel Processing Technology. 91 (2010) 322–328.

[11] W.W.S. Ho, H.K. Ng, S. Gan, S.H. Tan, Evaluation of palm oil mill fly ash supported calcium oxide as a heterogeneous base catalyst in biodiesel synthesis from crude palm oil, Energy Conversion and Management. 88 (2014) 1167–1178.

[12] M. Kaur, A. Ali, Ethanolysis of waste cottonseed oil over lithium impregnated calcium oxide: Kinetics and reusability studies, Renewable Energy. 63 (2014) 272–279.

[13] P. Kutálek, L. Čapek, L. Smoláková, D. Kubička, Aspects of Mg-Al mixed oxide activity in transesterification of rapeseed oil in a fixed-bed reactor, Fuel Processing Technology. 122 (2014) 176–181.

[14] M. Kouzu, T. Kasuno, M. Tajika, Y. Sugimoto, S. Yamanaka, J. Hidaka, Calcium oxide as a solid base catalyst for transesterification of soybean oil and its application to biodiesel production, Fuel. 87 (2008) 2798–2806.

[15] W. Tao, Y. Ping, W. Shenggang, L. Yunbai, Application of sodium aluminate as a heterogeneous base catalyst for biodiesel production from soybean oil, Energy and Fuels. 23 (2009) 1089–1092.

[16] H. V. Lee, J.C. Juan, Y.H. Taufiq-Yap, P.S. Kong, N.A. Rahman, Advancement in heterogeneous base catalyzed technology: An efficient production of biodiesel fuels, Journal of Renewable and Sustainable Energy. 7 (2015) 32701–46.

[17] A.P.S. Dias, J. Bernardo, P. Felizardo, M.J.N. Correia, Biodiesel production by soybean oil methanolysis over SrO/MgO catalysts: The relevance of the catalyst granulometry, Fuel Processing Technology. 102 (2012) 146–155.

[18] X. Deng, Z. Fang, Y. hu Liu, C.L. Yu, Production of biodiesel from Jatropha oil catalyzed by nanosized solid basic catalyst, Energy. 36 (2011) 777–784.

[19] S. Ismail, A. S. Ahmed, R. Anr, S. Hamdan, Biodiesel Production from Castor Oil by Using Calcium Oxide Derived from Mud Clam Shell, Journal of Renewable Energy. 2016 (2016) 1–8

[20] Y.H. Taufiq-Yap, H.V. Lee, M.Z. Hussein, R. Yunus, Calcium-based mixed oxide catalysts for methanolysis of *Jatropha curcas* oil to biodiesel, Biomass and Bioenergy. 35 (2011) 827-834.

[21] R. Luque, A. Pineda, J.C. Colmenares, J.M. Campelo, A.A. Romero, J.C. Serrano-Riz, L.F. Cabeza, J. Cot-Gores, Carbonaceous residues from biomass gasification as catalysts for biodiesel production, Journal of Natural Gas Chemistry. 21 (2012) 246–250.

[22] P.L. Boey, G.P. Maniam, S.A. Hamid, D.M.H. Ali, Utilization of waste cockle shell (Anadara granosa) in biodiesel production from palm olein: Optimization using response surface methodology, Fuel. 90 (2011) 2353–2358.

General Conclusions

Overall, this research has achieved the following:

- Heterogeneous base catalysts were successfully synthesized from red mud using soda-lime calcination.
- Modification of red mud using soda-lime calcination gave significant influence on its crystallinity, morphology, specific surface area, and produced active sites, such as sodium aluminate ($NaAlO_4$) and sodium carbonate ($Na_2Si_2O_5$) which showed high basicity and selectivity to produce biodiesel.
- The catalyst showed good performance as solid base catalyst for transesterification of canola oil which resulted in 99.6% FAME yield under the following conditions: 12:1 methanol/oil molar ratio, 4 wt% catalyst concentration, 60°C reaction temperature, and 2 h reaction time.
- Deactivation of modified red mud catalyst used in transesterification reaction might be caused by several factors, but mainly is due to deposits of organic compounds on the catalyst.
- The regeneration by washing with hexane and calcination can recover its catalytic activity close to that of the fresh one.

List of Publications

Journal

A. Wahyudi, W. Kurniawan and H. Hinode, **Modification of red mud (bauxite residue) into sponge base catalyst through soda-lime calcination,** Int. J. Adv. Sci. Eng. Technol., 4 (1) spcl. Iss-3, 9–12 (2016).

A. Wahyudi, W. Kurniawan and H. Hinode, **Utilization of modified red mud as a heterogeneous base catalyst for transesterification of canola oil,** J. Chem. Eng. Jpn., 50 (7), 561-567 (2017).

A. Wahyudi, W. Kurniawan and H. Hinode, **Study on deactivation and regeneration of modified red mud catalyst used in biodiesel production,** J. Green Sustain. Chem., (accepted)

Conference and Workshop

2nd Green and Sustainable Chemistry Conference
May 14-17, 2017, Berlin, Germany
"High yield biodiesel production by modified red mud catalyst"

Workshop on The Utilization of Waste Materials
September 4-5, 2015, Manila, Philippines
"Potential applications of red mud (bauxite residue) in Indonesia"

Joint Workshop of Beihang Univ. – Tokyo Tech. on Nano/Micro-Engineering
October 25-27, 2015, Beijing, China
"Conversion of red mud (bauxite residue) into base catalyst for biodiesel production"

Acknowledgments

The author would like to express his sincerest gratitude and deepest thanks to those whose valuable contributions and assistance have helped the realization of this research:

To my adviser, Prof. Hirofumi Hinode, and assistant professor Dr. Winarto Kurniawan, for their continuous support for my research. I will forever be thankful for all the knowledge, motivation, guidance and patience you have given to me.

The members of the doctoral examination committee, Prof. Kunio Yoshikawa, Prof. Fumitake Takahashi, Prof. Ryuichi Egashira, and Dr. Eden Mariquit, for the time and efforts, their questions and comments which helped improve this thesis.

To the Monotsukuri Center of Tokyo Institute of Technology, especially for the assistance of Ms. Takako Kanai, person-in-charge for some analytical instruments (Autosorb and SEM). I am also grateful for the assistance of Mr. Vo Thanh Phuoc, PhD student of Yoshikawa-lab, for patiently teaching me how to use GC-MS.

To the members of Hinode Laboratory, for their warm reception and for all their valuable insights and contributions which helped me during my research, particularly through the discussions throughout the laboratory seminars.

To my institution in Indonesia, R&D Center for Mineral and Coal Technology (*tek*MIRA), for the support and assistance, especially for preparing all the things related to the administration and technical purposes for my study in Japan.

To my family for the support they have provided me in my decisions, and endeavors, and for always being there for me. To my friends and Indonesian community in Tokyo, whose support has helped me overcome any problems I have encountered and has kept me sane.

Finally, I would like to acknowledge the financial support given by the

Ministry of Energy and Mineral Resources, Republic of Indonesia, for offering the scholarship.